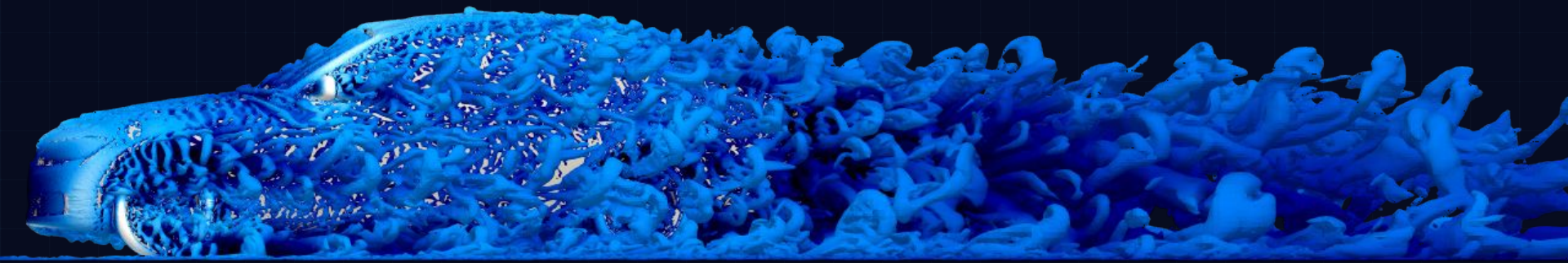
5th Automotive CFD Prediction Workshop

Scale-resolving OpenFOAM simulations of DriveAer test case using dynamic eddy viscosity RANS closure

8–9 October 2026 • DAMA Technopole, Bologna, Italy



R. Aluzzi G. Manzi A. Cimarelli

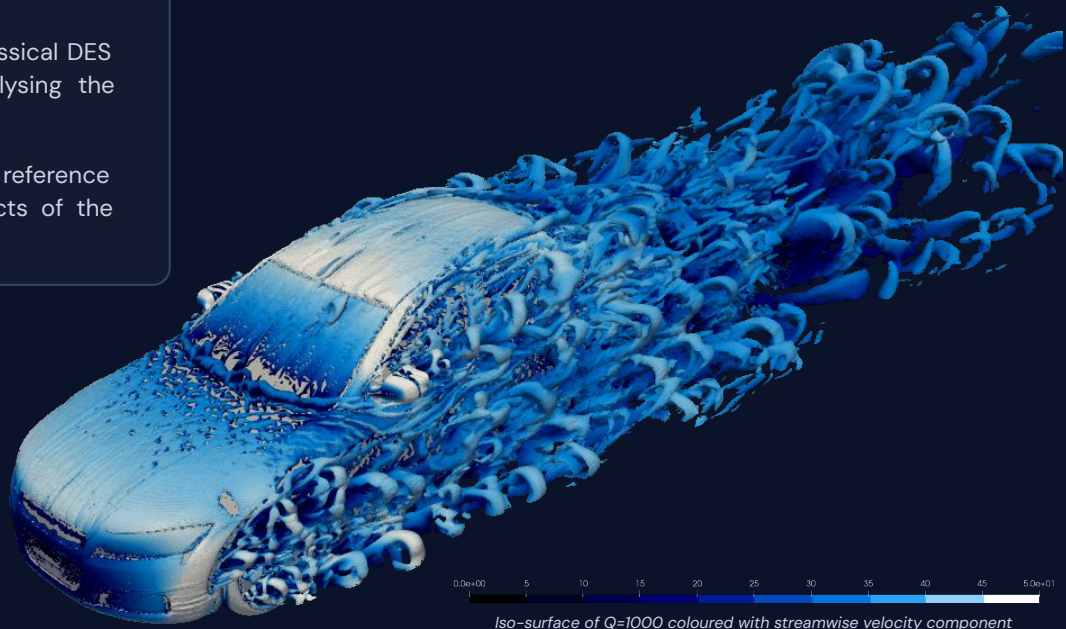
Introduction & Motivation

Motivation & Research Objective

The turbulence model: a novel scale-resolving turbulence closure, based on temporal filtering coupled with a dynamic procedure, has been developed and tested on canonical flows (e.g., T3L, periodic channels with bump, BARC, NACA airfoil).

The target: evaluate the model's potential as an alternative to classical DES formulations on complex industrial benchmark particularly analysing the robustness to temporal discretization coarsening.

The methodology: unsteady simulations campaign employ the reference grids provided by the organizing committee to isolate the effects of the closure model.



Iso-surface of Q=1000 coloured with streamwise velocity component

Numerics & Solver Setup

Solver

- **Simulation Software:** OpenFOAM v10
- **Solver:** Segregated PIMPLE algorithm
- **Turbulence Model:** Dynamic Eddy Viscosity k-ω Zero-Decay

Mesh and cases:

- **Mesh:** ANSA hi-Re (ACFD5) coarse (60M) and baseline (120M)
- **Cases:** both 2a and 2b for coarse while only 2a for baseline

Numerical Schemes

- **Time integration:** backward
- **Convection (velocity):** Gauss linearUpwindV
- **Convection (turbulence):** bounded Gauss linearUpwind
- **Gradient:** leastSquares for pressure; cellLimited Gauss linear 1 for turbulence

Temporal Sensitivity Analysis

To evaluate robustness of the turbulence model under coarsening the temporal resolution, four different time step are tested:

Case name	Δt	***Averaging over***
coarse x1	1e-04	[0.7, 3] sec
coarse x10	1e-03	[0.7, 3] sec
coarse x20	2e-03	[1, 6] sec
coarse x50	5e-03	[1, 6] sec
baseline x1	1e-04	[0.5, 3] sec
baseline x10	1e-03	[0.5, 3] sec
baseline x20	2e-03	[0.5, 3] sec
baseline x50	5e-03	[0.5, 3] sec

Theoretical Framework

The time filtering formalism can be introduced to get a more general paradigm for hybrid approaches [1,2]:

Temporally filtered Navier-Stokes equations

$$\frac{\partial \langle u_i \rangle_\tau}{\partial x_i} = 0 \qquad R_\tau(u_i,u_j) = \langle u_i u_j \rangle_\tau - \langle u_i \rangle_\tau \langle u_j \rangle_\tau \neq -2\nu_\tau \langle S_{ij} \rangle_\tau$$

$$\frac{\partial \langle u_i \rangle_\tau}{\partial t} + \frac{\partial \langle u_i \rangle_\tau \langle u_j \rangle_\tau}{\partial x_j} = -\frac{1}{\rho}\frac{\partial \langle p \rangle_\tau}{\partial x_i} + \nu \frac{\partial^2 \langle u_i \rangle_\tau}{\partial x_j \partial x_j} - \frac{\partial R_\tau(u_i,u_j)}{\partial x_j}$$

Double filtering formalism[3]



HYBRID: TEMPORAL FILTER

Germano's identity[4] in temporal framework:

$$R_{T_\tau}(u_i,u_j) - \langle R_\tau(u_i,u_j)\rangle_T = \langle \langle u_i \rangle_\tau \langle u_j \rangle_\tau \rangle_T - \langle \langle u_i \rangle_\tau \rangle_T \langle \langle u_j \rangle_\tau \rangle_T$$

Eddy Viscosity Models

Boussinesq assumption:

$$R_\tau(u_i,u_j) = -2\nu_\tau \langle S_{ij} \rangle_\tau$$
$$R_{T_\tau}(u_i,u_j) = -2\nu_{T_\tau} \langle \langle S_{ij} \rangle_\tau \rangle_T$$

k-ω formalism:

$$\begin{cases} \nu_\tau = \dfrac{C_\mu}{\beta^*}\dfrac{k_\tau}{\omega_\tau} \\ \nu_{T_\tau} = \dfrac{C_\mu}{\beta^*}\dfrac{k_{T_\tau}}{\omega_{T_\tau}} \end{cases}$$

The quantity associated to the coarser filter level are not transported, rather can be computed as [3]:

$$\begin{cases} k_{T_\tau} = \dfrac{1}{2}\langle k_\tau \rangle_T + \dfrac{1}{2}\mathcal{L}_{ii} \\ \epsilon_{T_\tau} = \langle \epsilon_\tau \rangle_T + \nu \mathcal{D}_{ii} \end{cases}$$

$$\omega_{T_\tau} = \frac{1}{k_{T_\tau}}\left(\langle k_\tau \omega_\tau \rangle_T + \frac{\nu}{\beta^*}\mathcal{D}_{ii} \right)$$

The two tensor take origin from the same algebraic properties introduced by the use of filtering formalism when comparing hierarchically organized filter levels:

$$\mathcal{L}_{ij} \equiv R_T(u_i,u_j) - \langle R_\tau(u_i,u_j)\rangle_T = \langle \langle u_i \rangle_\tau \langle u_j \rangle_\tau \rangle_T - \langle \langle u_i \rangle_\tau \rangle_T \langle \langle u_j \rangle_\tau \rangle_T$$

$$\mathcal{D}_{ij} \equiv R_T\left(\frac{\partial u_i}{\partial x_j}, \frac{\partial u_i}{\partial x_j}\right) - \left\langle R_\tau\left(\frac{\partial u_i}{\partial x_j}, \frac{\partial u_i}{\partial x_j}\right)\right\rangle_T = \left\langle \frac{\partial \langle u_i \rangle_\tau}{\partial x_j}\frac{\partial \langle u_i \rangle_\tau}{\partial x_j} \right\rangle_T - \frac{\partial \langle \langle u_i \rangle_\tau \rangle_T}{\partial x_j}\frac{\partial \langle \langle u_i \rangle_\tau \rangle_T}{\partial x_j}$$

[1] Pruett et al., Temporal large-eddy simulation: theory and implementation, TCFD (2008).
[2] Fadai-Ghotbi et al., Temporal filtering: a consistent formalism for seamless hybrid RANS-LES modeling in inhomogeneous turbulence, IJHFF (2010).
[3] Cimarelli et al., Unifying formalism and closures for coarse-grained approaches to turbulence, PoF (2026).
[4] Germano, M. 1992 Turbulence: the filtering approach. J. Fluid Mech. 238, 325–336.

Theoretical Framework

Dynamic procedure

Substituting all inside the Germano's identity we get the following tensorial system:

$$2\frac{C_\mu}{\beta^*}\left\langle\frac{k_\tau}{\omega_\tau}\langle S_{ij}\rangle_\tau\right\rangle_T - 2\frac{C_\mu}{\beta^*}\frac{k_{T_\tau}}{\omega_{T_\tau}}\langle\langle S_{ij}\rangle_\tau\rangle_T = \langle\langle u_i\rangle_\tau\langle u_j\rangle_\tau\rangle_T - \langle\langle u_i\rangle_\tau\rangle_T\langle\langle u_j\rangle_\tau\rangle_T$$

which equivalently reads:

$$C_\mu \mathcal{Z}_{ij} = \mathcal{L}_{ij}$$

$$\mathcal{Z}_{ij} = \left[\frac{2}{\beta^*}\left\langle\frac{k_\tau}{\omega_\tau}\langle S_{ij}\rangle_\tau\right\rangle_T - \frac{2}{\beta^*}\frac{k_{T_\tau}}{\omega_{T_\tau}}\langle\langle S_{ij}\rangle_\tau\rangle_T\right]$$

solvable using square error minimization[4]

$$C_\mu = \frac{\mathcal{L}_{ij}\mathcal{Z}_{ij}}{\mathcal{Z}_{kl}\mathcal{Z}_{kl}}$$

Zero-decay modification

According to Spalart[5], classical eddy viscosity models exhibit non-physical decay of turbulent quantities under free-stream conditions described, for the k-ω formulation, by the following set of equations:

$$\left.\begin{aligned} k(x) &= k_{in}\left[1+\beta\,\omega_{in}\frac{x}{U_\infty}\right]^{-\frac{\beta^*}{\beta}} \\ \omega(x) &= \frac{\omega_{in}}{1+\beta\,\omega_{in}\frac{x}{U_\infty}} \end{aligned}\right\}$$

Using the new information about the solution we can introduce an additional coefficient in the destruction term both for k and ω leading to a no free-stream decay formulation:

$$C_\mu^* = \left(\frac{C_\mu}{C_{\mu_{base}}}\right) \rightarrow \frac{Dk_\tau}{Dt} = -C_\mu^*\beta^* k_\tau\omega_\tau \quad ; \quad \frac{D\omega_\tau}{Dt} = -C_\mu^*\beta\omega_\tau^2$$

$$\begin{aligned} \frac{\partial k_\tau}{\partial t} + \frac{\partial k_\tau\langle u_j\rangle_\tau}{\partial x_j} &= 2\nu_t\langle S_{ij}\rangle_\tau\langle S_{ij}\rangle_\tau - C_\mu^*\beta^* k_\tau\omega_\tau + \frac{\partial}{\partial x_j}\left[\left(\nu+\frac{\nu_t}{\sigma_k}\right)\frac{\partial k_\tau}{\partial x_j}\right] \\ \frac{\partial \omega_\tau}{\partial t} + \frac{\partial \omega_\tau\langle u_j\rangle_\tau}{\partial x_j} &= 2\gamma\frac{\omega_\tau}{k_\tau}\nu_t\langle S_{ij}\rangle_\tau\langle S_{ij}\rangle_\tau - C_\mu^*\beta\omega_\tau^2 + \frac{\partial}{\partial x_j}\left[\left(\nu+\frac{\nu_t}{\sigma_\omega}\right)\frac{\partial \omega_\tau}{\partial x_j}\right] \end{aligned}$$

[4] Lilly, D.K. 1992 A proposed modification of the germano subgrid-scale closure method. Phys. Fluids A 4, 633–635.
[5] Philippe R. Spalart Christopher L. Rumsey Effective Inflow Conditions for Turbulence Models in Aerodynamic Calculations. AIAA Journal vol. 45 No 10 Oct. 2007.

Theoretical Framework

Documentation

An exhaustive analysis of the model, from its analytical derivation to future perspectives, is discussed in detail in our recent publications:



*A. Cimarelli, N. Marras, B. Niceno, and Y. Tessier Urrecha, "**Unifying formalism and closures for coarse-grained approaches to turbulence**", Phys. Fluids 38(7), 075125 (2026). https://doi.org/10.1063/5.0332795*

*Y. Tessier Urrecha, G. Manzi, F. Cancellotti, and A. Cimarelli, "**Development of a class of dynamic RANS closures for coarse-grained approaches to turbulence**", submitted to Flow, Turbulence and Combustion (under review), 2026. Preprint available at arXiv:2610.03067.*

Resources

The C++ implementation of dynamic k - ω model, compatible with OpenFOAM v10 and v13, is available on the following GitHub repository:



https://github.com/GiorgioManzi/DynamicEddyViscosity.git

Contacts

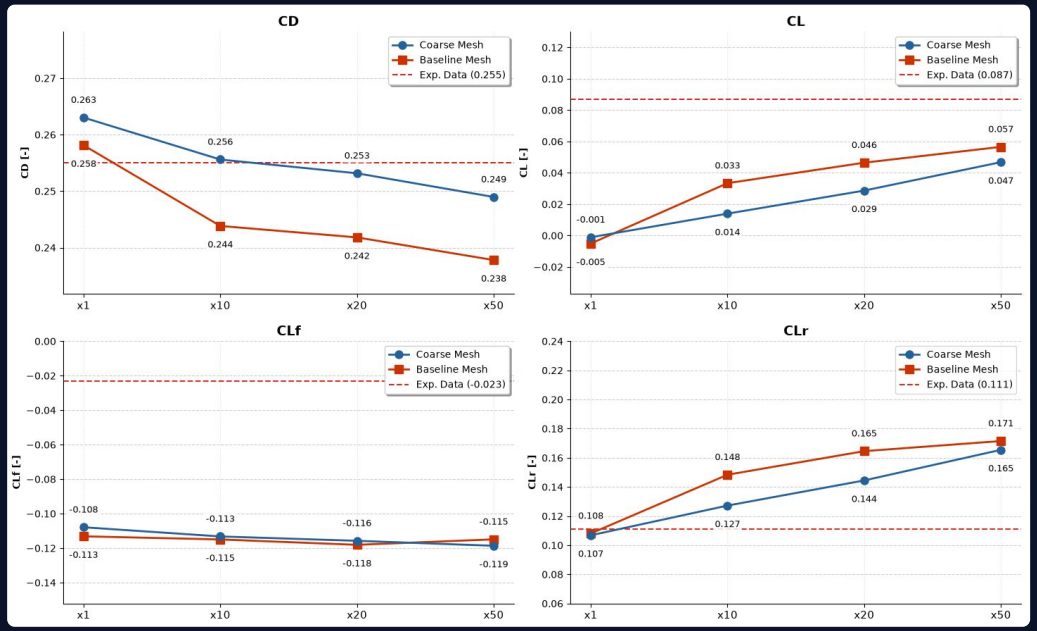
We encourage the CFD community to test the model on new industrial benchmarks. For questions and feedback feel free to reach out.

andrea.cimarelli@unimore.it

giorgio.manzi@unimore.it

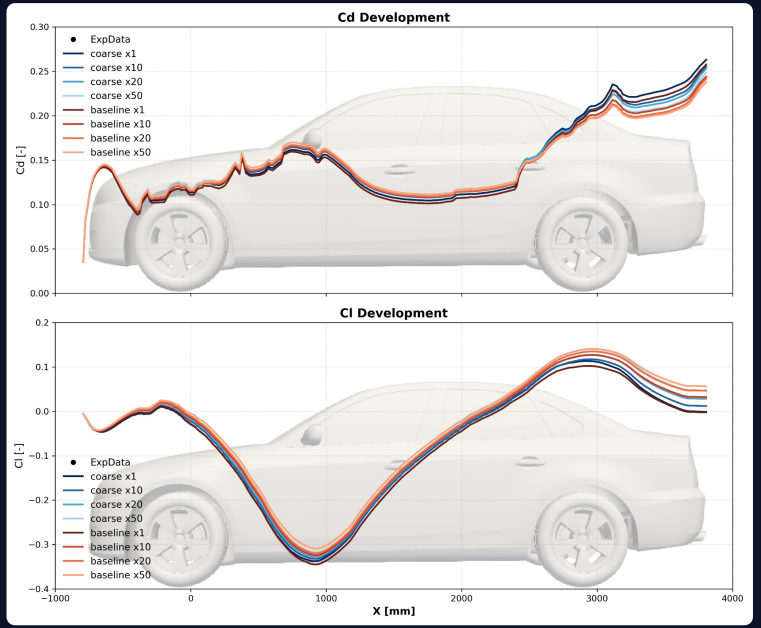
Results

Aerodynamic Coefficients and Developments



- Consistent Δt-induced trends across all coefficients for both mesh setups.
- Baseline mesh results show a clear drag coefficient underprediction at higher time steps.

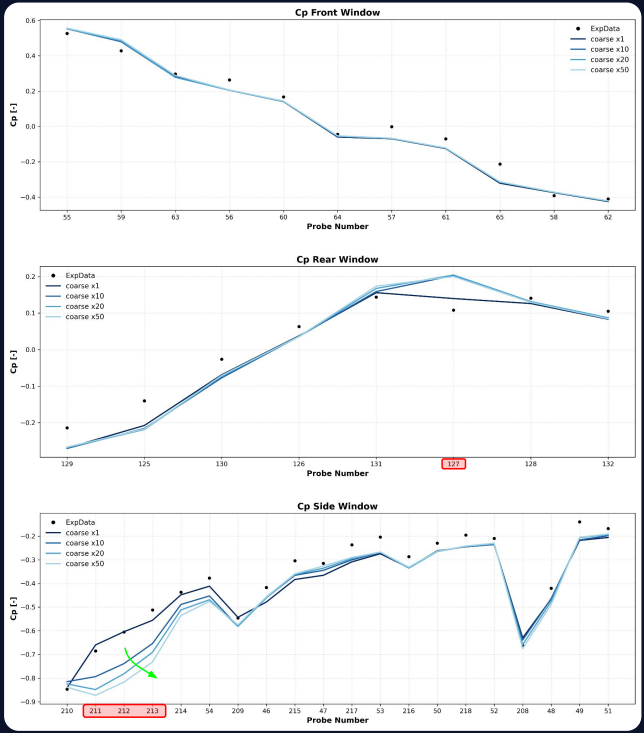
- Main deviations in the aerodynamic coefficient development are confined to the rear region.

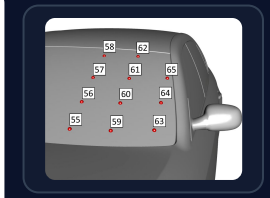


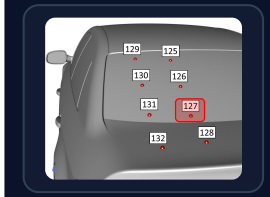
Where differences come from…

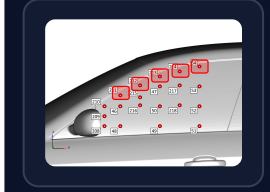


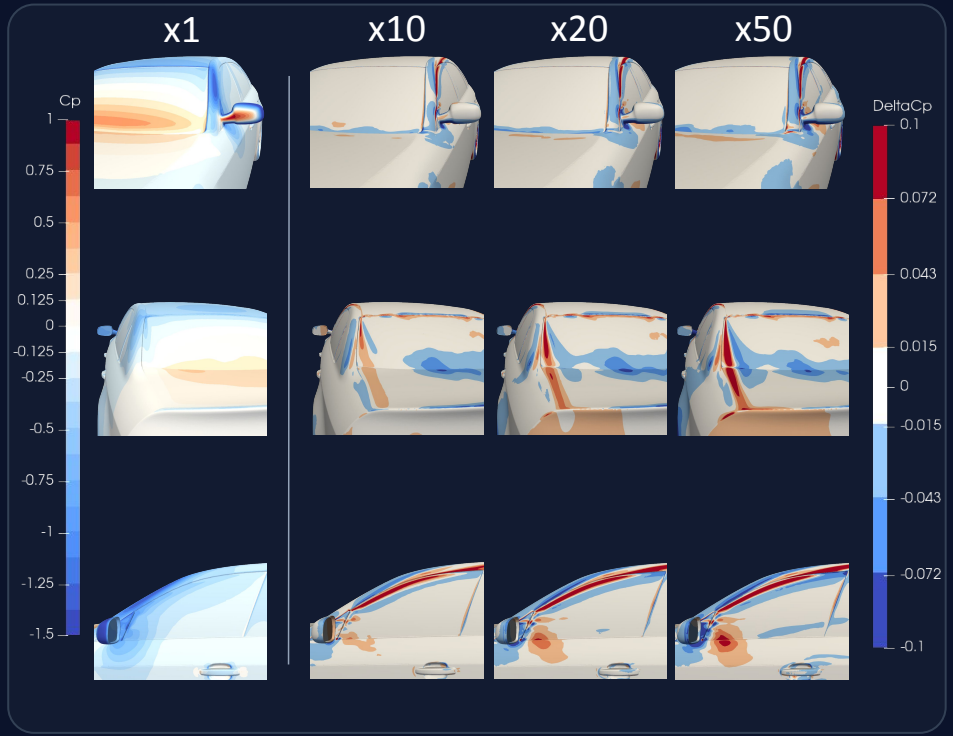
Surface Pressure — windows





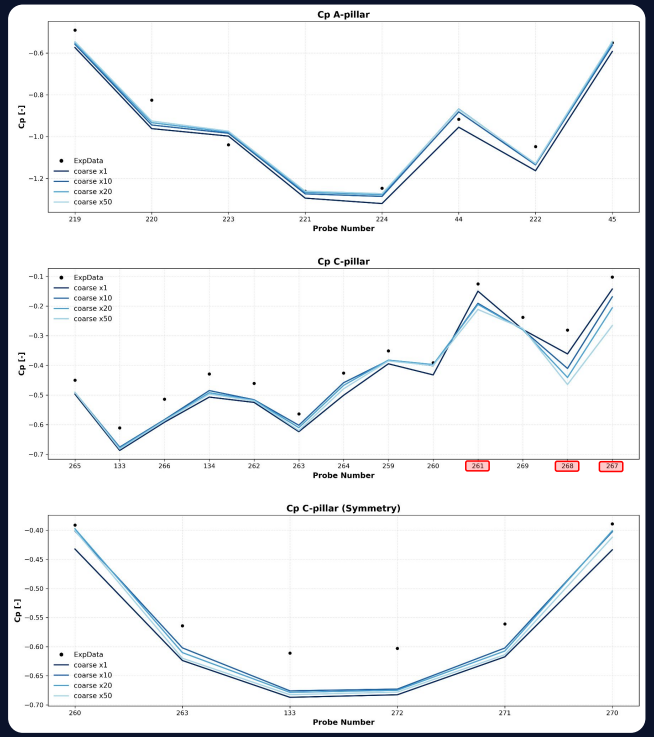


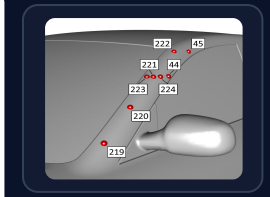


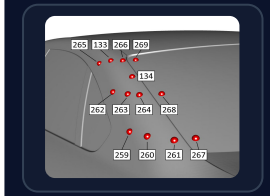


- Time step sensitivity is localized specifically on the upper part of the rear window.
- Elevated time steps result in an increase of suction footprint also on the mirrors.

Surface Pressure — pillars





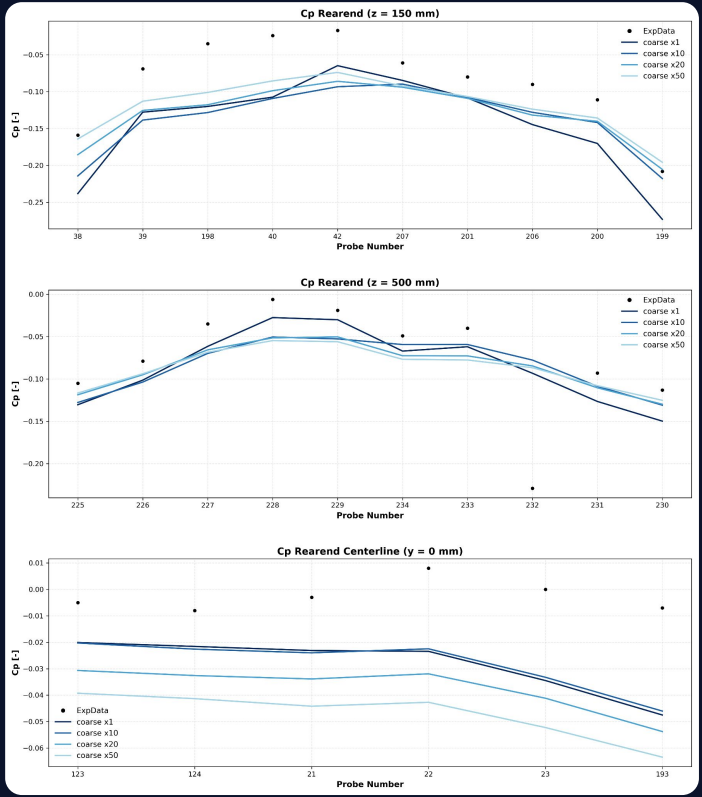


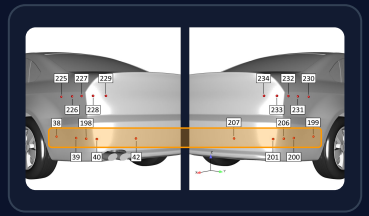


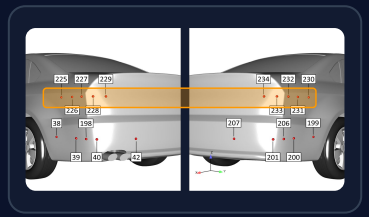


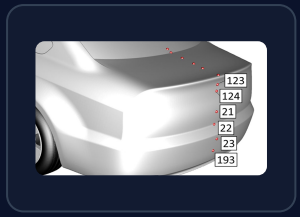
- The pressure distribution along the C-pillars exhibits a similar behaviour of the A-pillar.
- Same footprint of the A-pillar is also visible for the C-pillar.

Surface Pressure — rear end





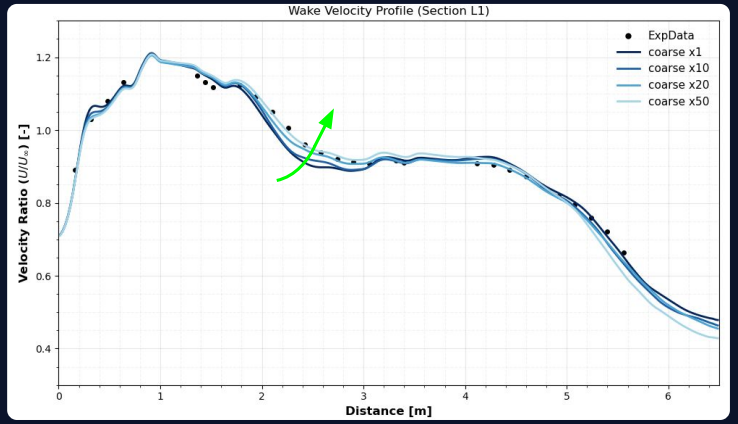


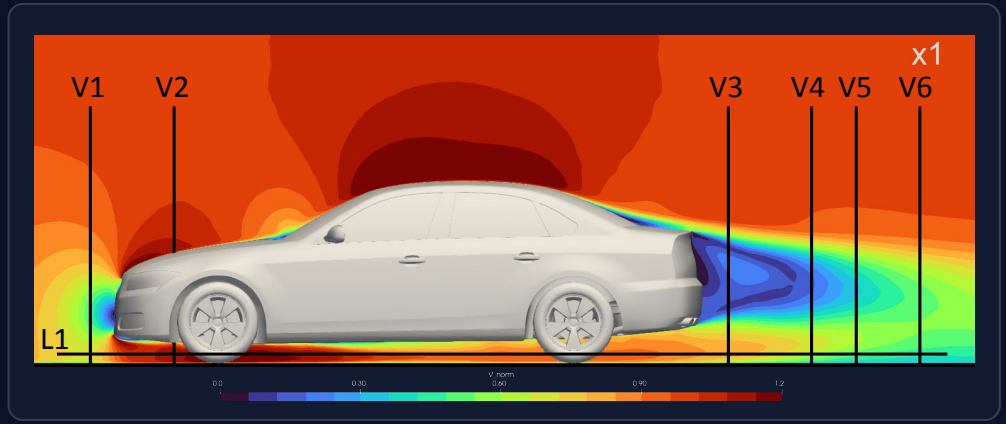


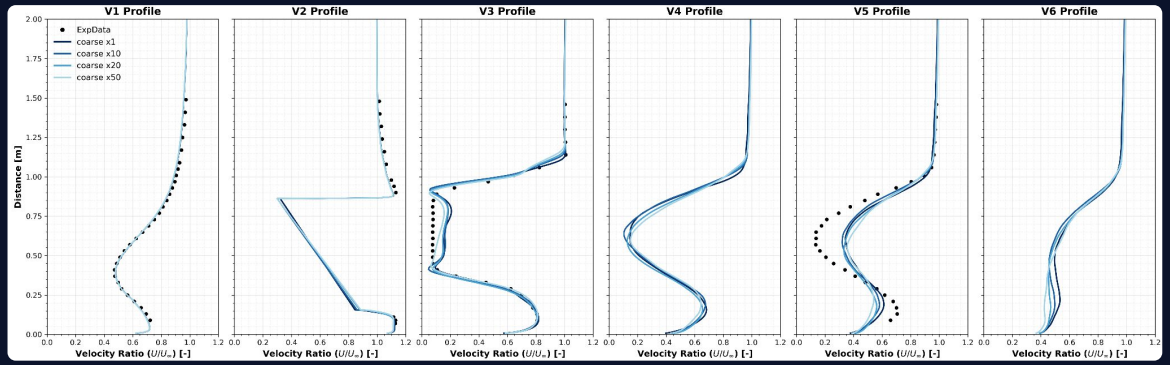


The model successfully captures the macroscopic trends and shape of the pressure distribution while exhibit underprediction of pressure recovery across the entire rear end.

L1 & V – profiles

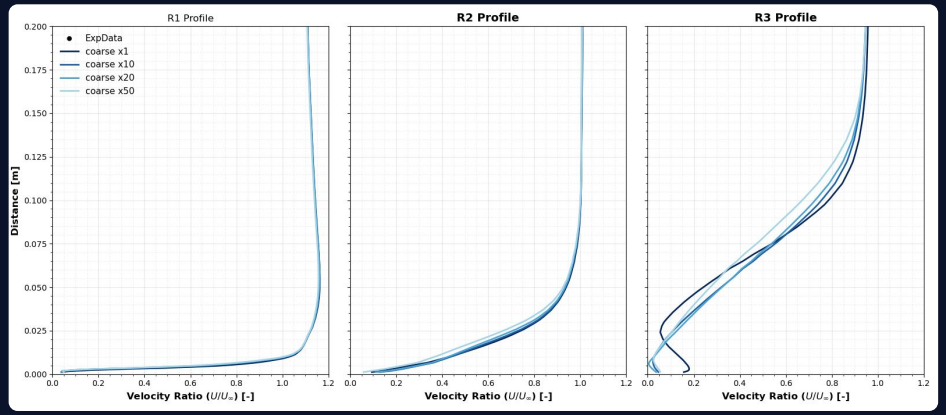




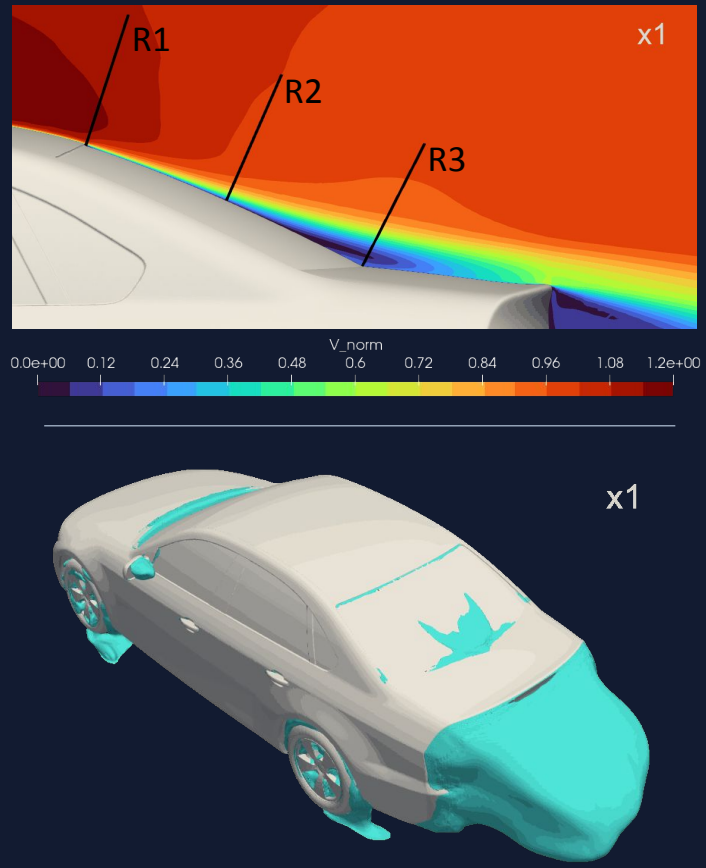


- ***V5 deficit:*** the velocity deficit characterizing the V5 profile is not fully captured by any simulation.
- ***V3 wake core:*** the simulation struggles to replicate the velocity plateau measured within the wake core.
- ***V3 shear layer spreading:*** velocity deficit observed above the primary shear layer.

R - profiles (rear window)

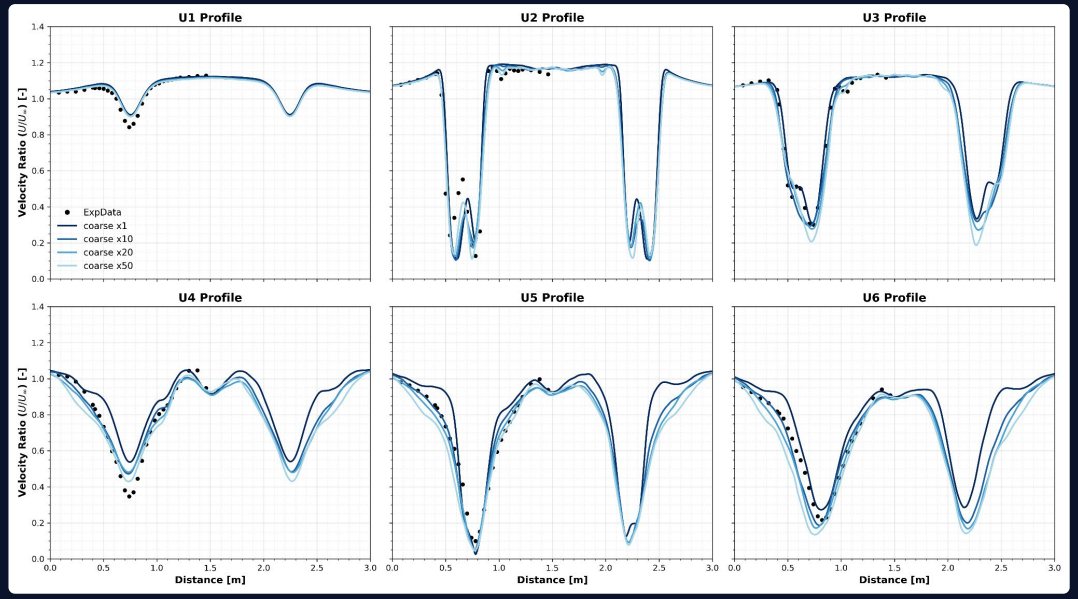


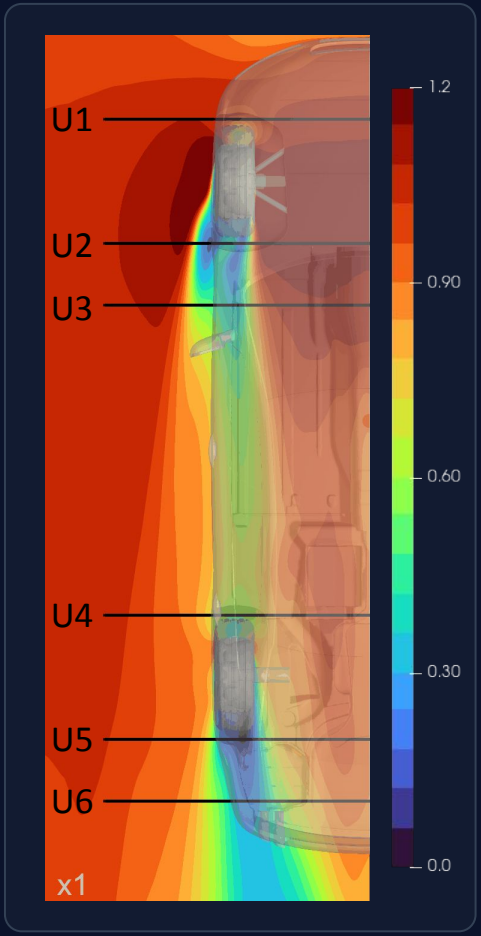
- Marked Δt-insensitivity for the attached boundary layer along the upper rear window (R1 and R2).
- Global separation topology remains consistent across all tested time steps.
- Increasing the time step promotes more pronounced flow separation evidenced on R3 velocity profile.
- Increasing the time step trigger the onset of a small, localized separation region downstream of the rear wheel on the bumper.



Iso-surface of normalized streamwise velocity Vx=0.

U - profiles

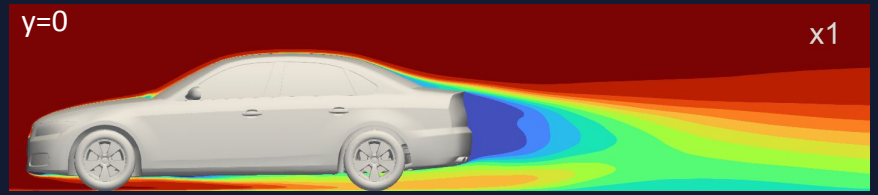


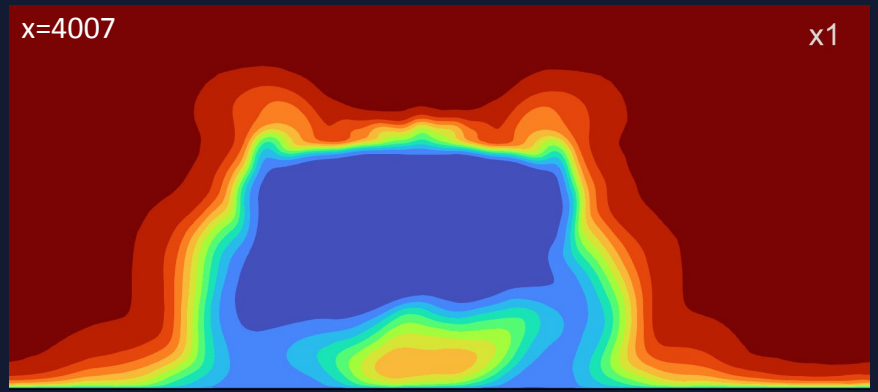


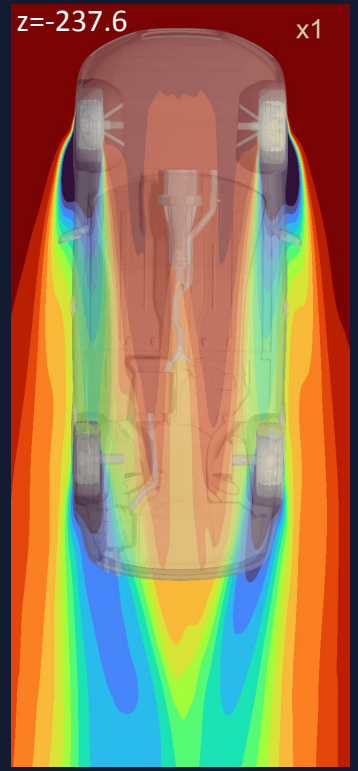
- Coarsening the temporal resolution leads to a downstream elongation of the tire wake, resulting in a marked momentum deficit clearly visible in profiles U3, U4 and U6.
- Counterintuitively the highest temporal coarsening levels yield the better agreement with wind tunnel reference data for profiles U2, U4 and U5.
- *T*he flow topology in the upstream section remains strictly Δt-insensitive visible in U1 profile.

Total pressure coefficient









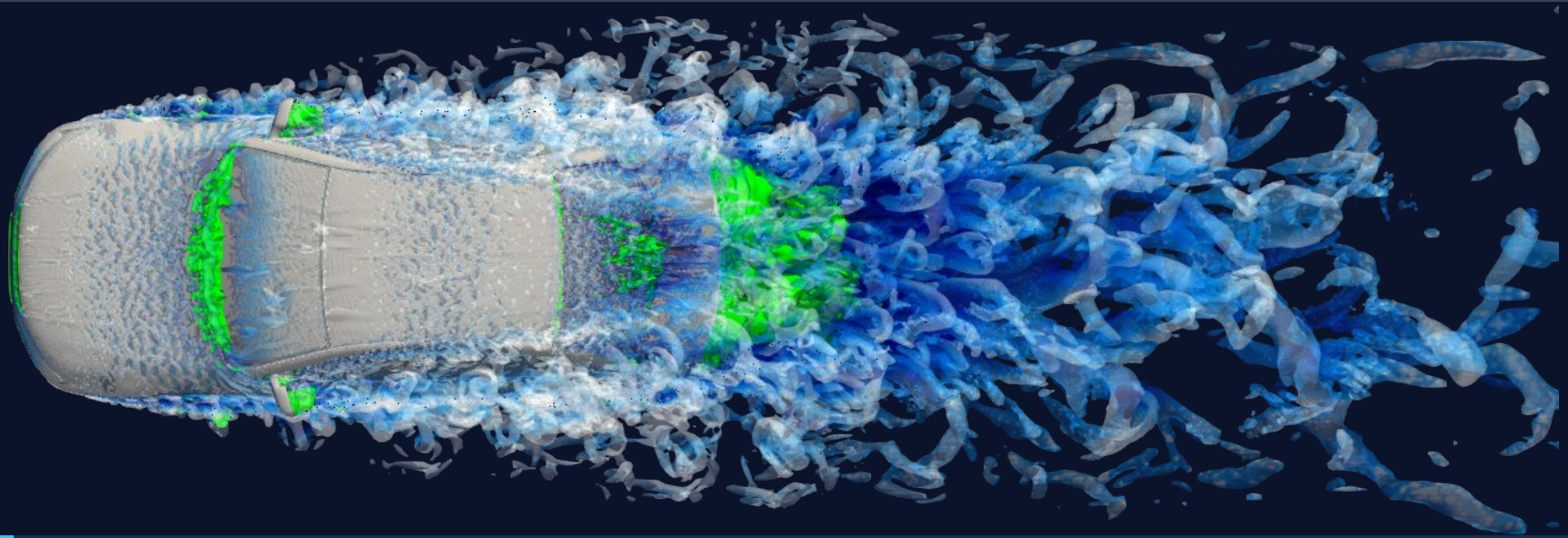


Conclusion

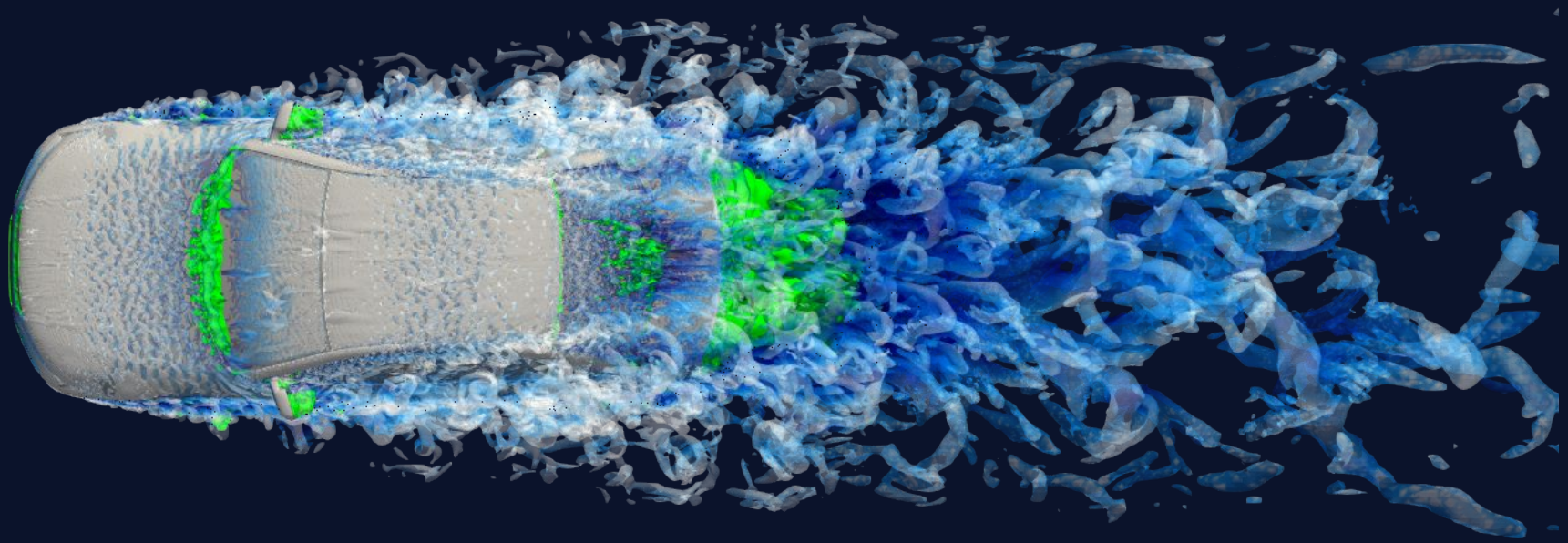
Robustness on industrial benchmark: the dynamic closure demonstrated a good capability to handle a complex industrial benchmark like the DriveAer, providing to be a viable alternative to classical DES formulation on coarse grids.

Temporal coarsening robustness: despite the severe coarsening of the time step, coupled with the coarser mesh available, a remarkably low degradation in the overall predictive accuracy is observed also operating at timestep x50 times larger (Δt=5e-03s) over the reference of Δt=1e-04.

Computational efficiency: the ability to employ very large timesteps coupled with coarse spatial discretization translates directly into reduction of the computational effort.



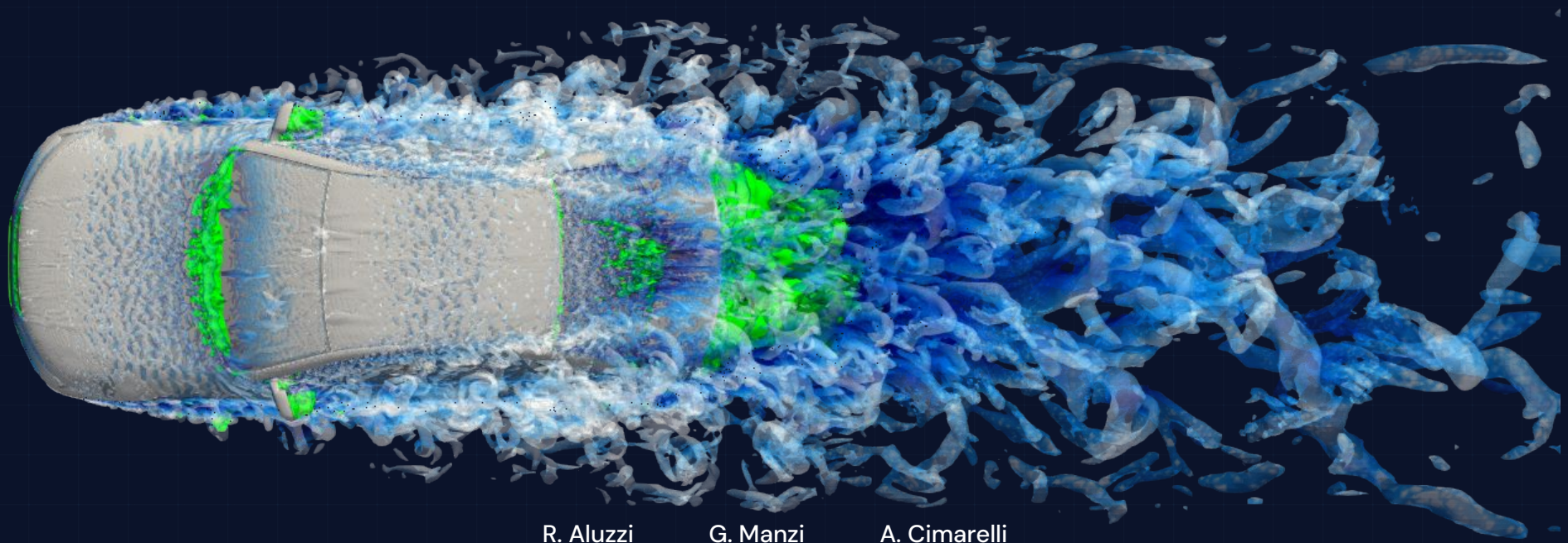
Thank you for your attention



5th Automotive CFD Prediction Workshop

Scale-resolving OpenFOAM simulations of DriveAer test case using dynamic eddy viscosity RANS closure

Additional Material



R. Aluzzi G. Manzi A. Cimarelli

Coarse Mesh

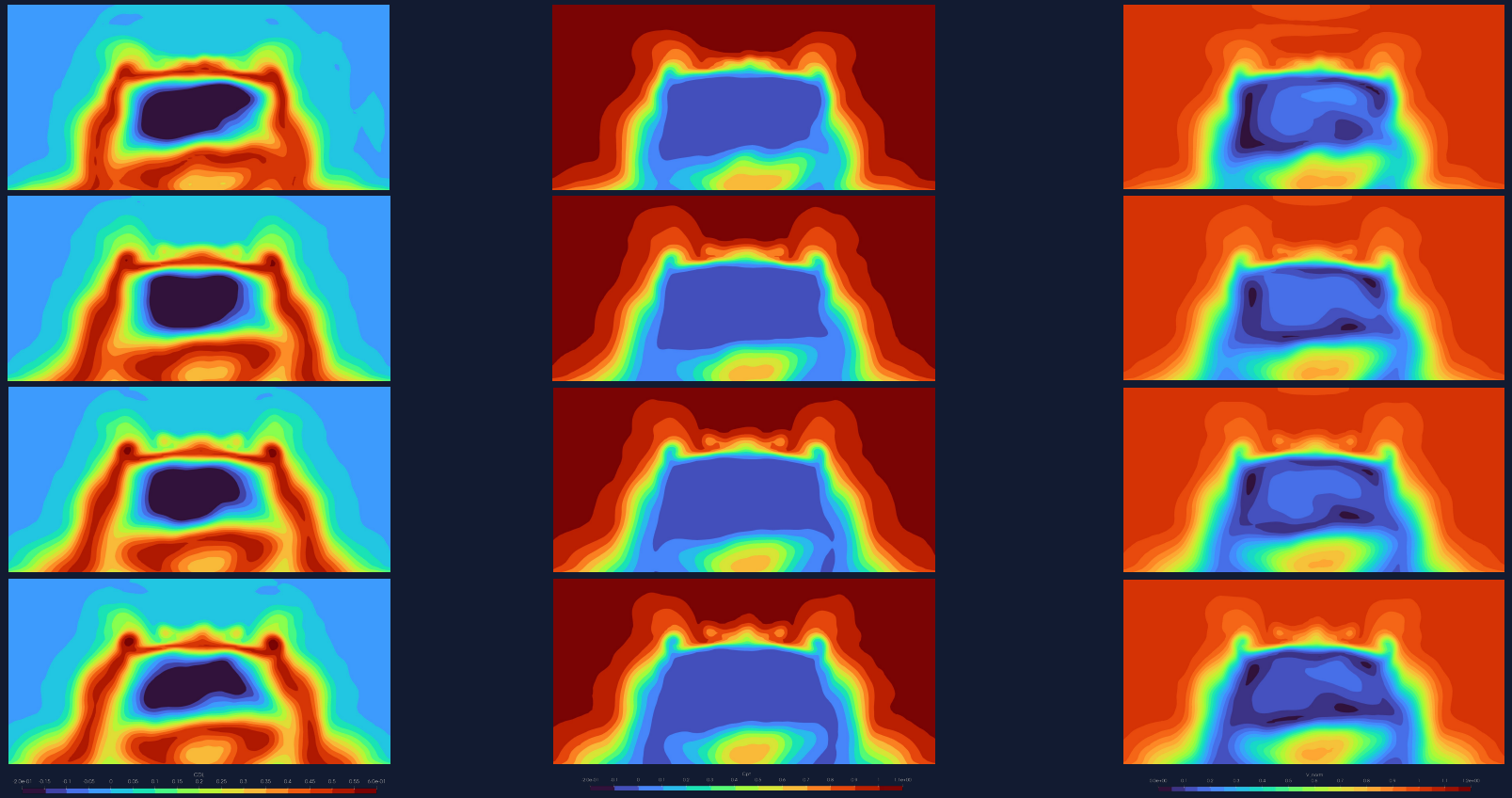
Flow Field — wake X

x1

x10

x20

x50



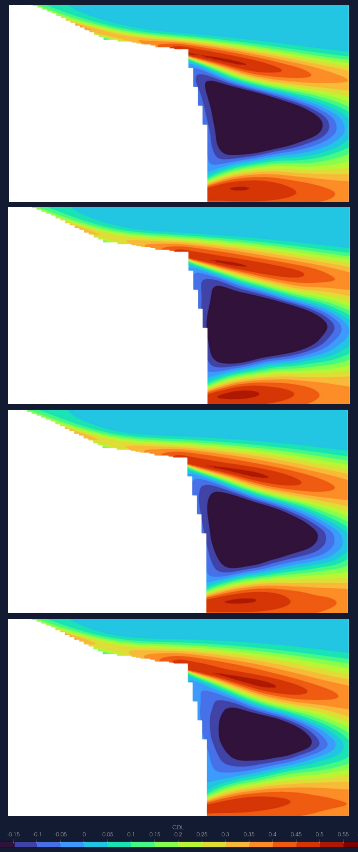
Flow Field — wake Y

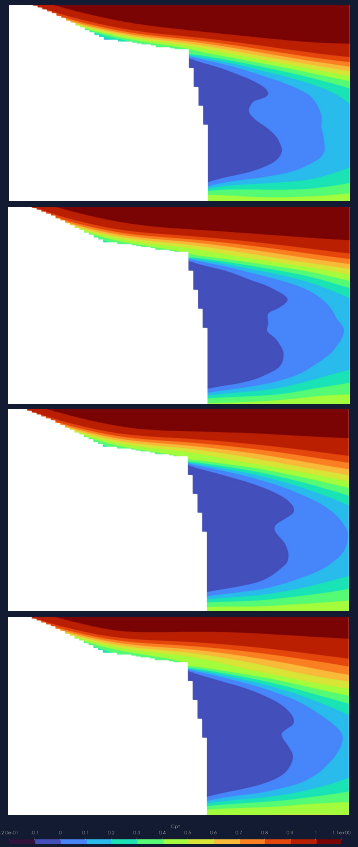
x1

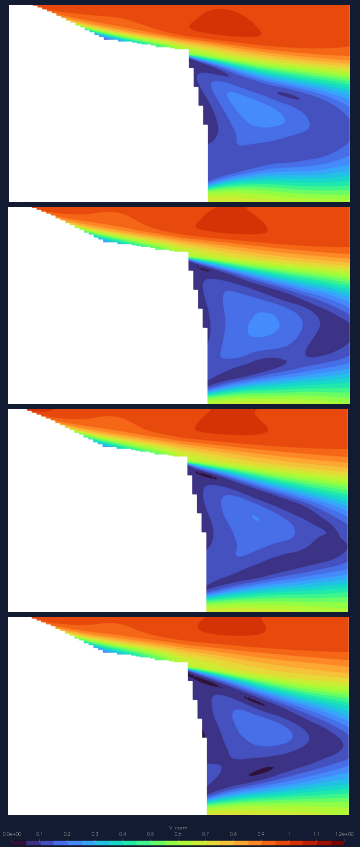
x10

x20

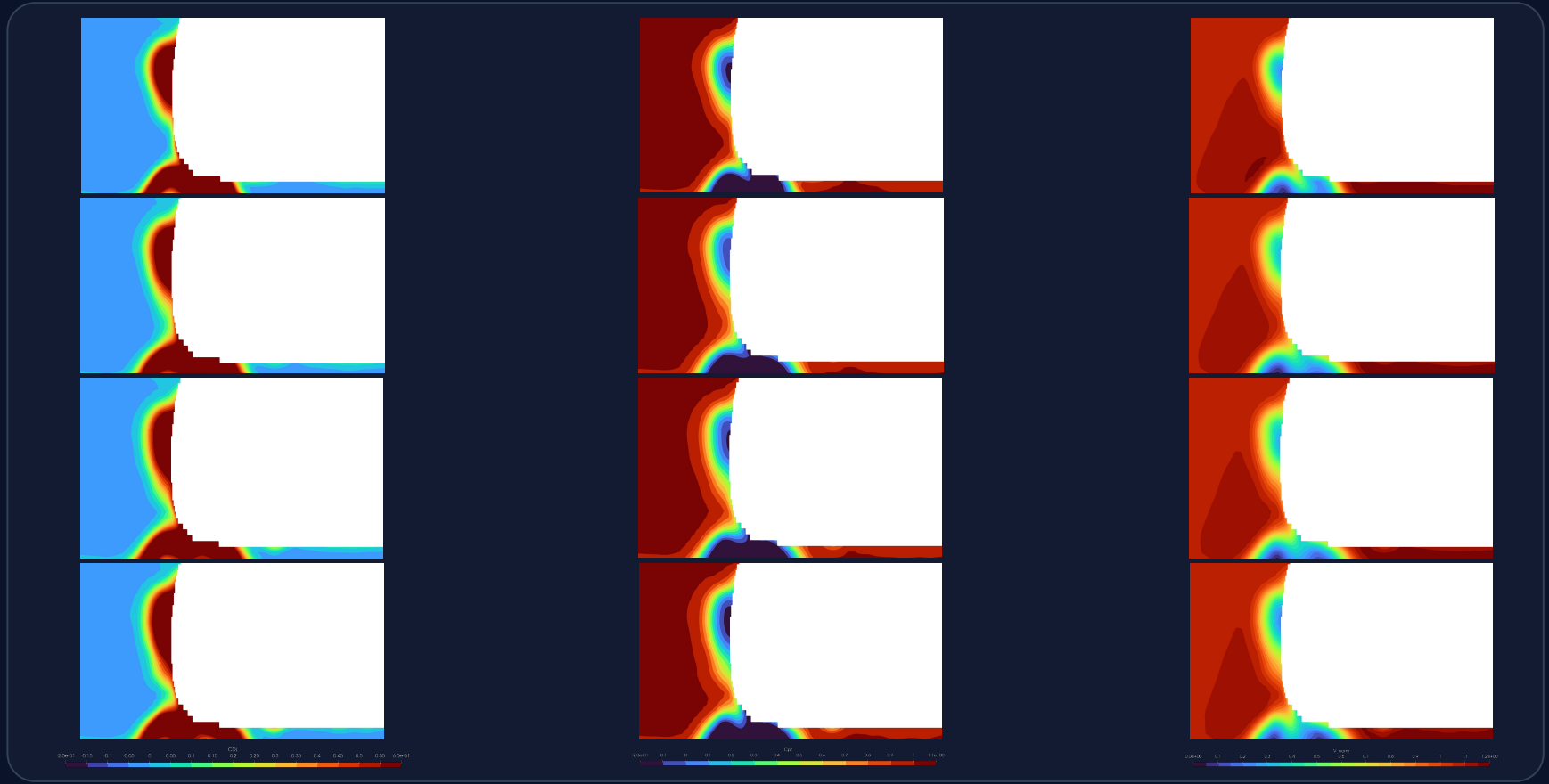
x50



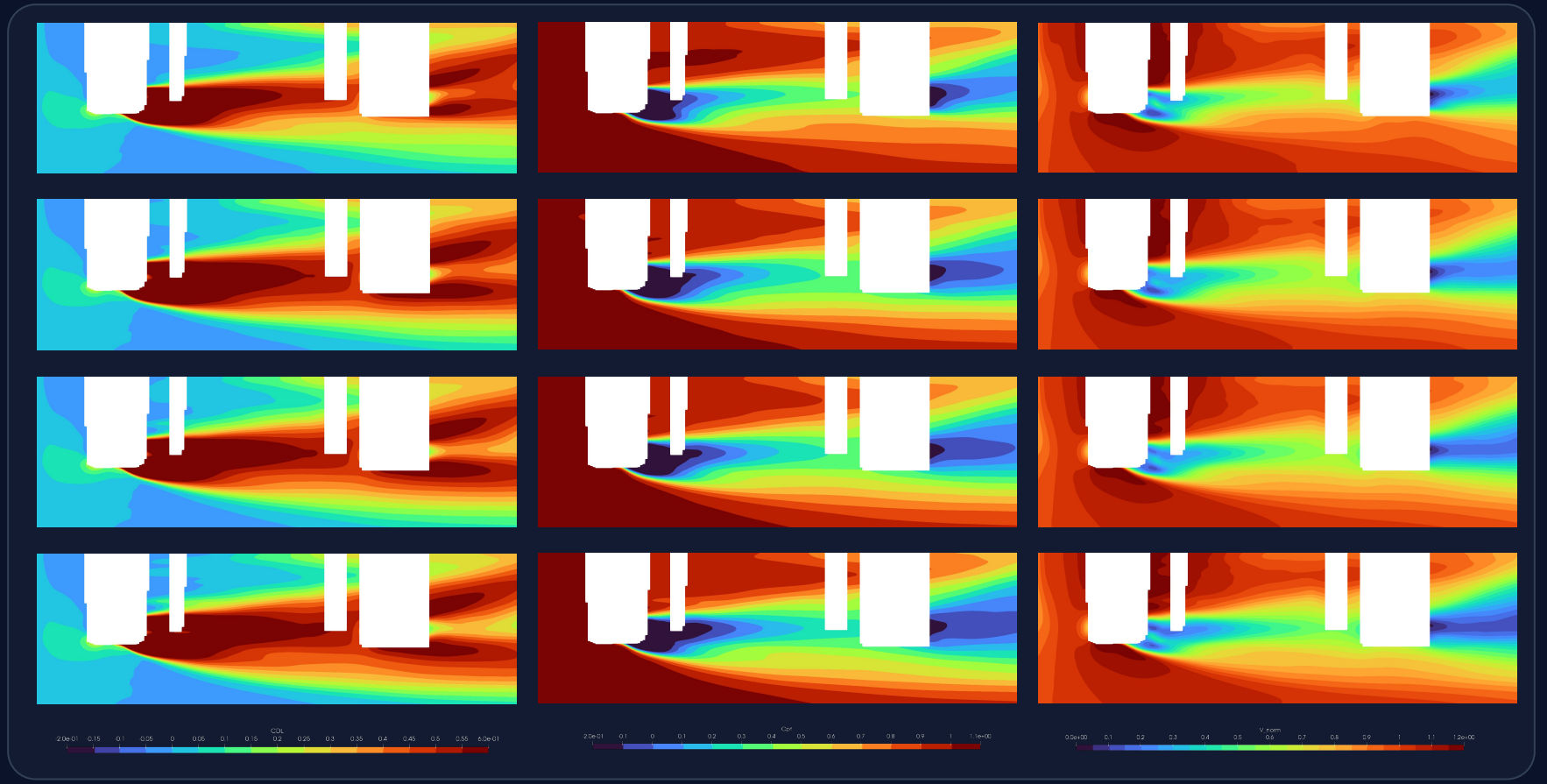




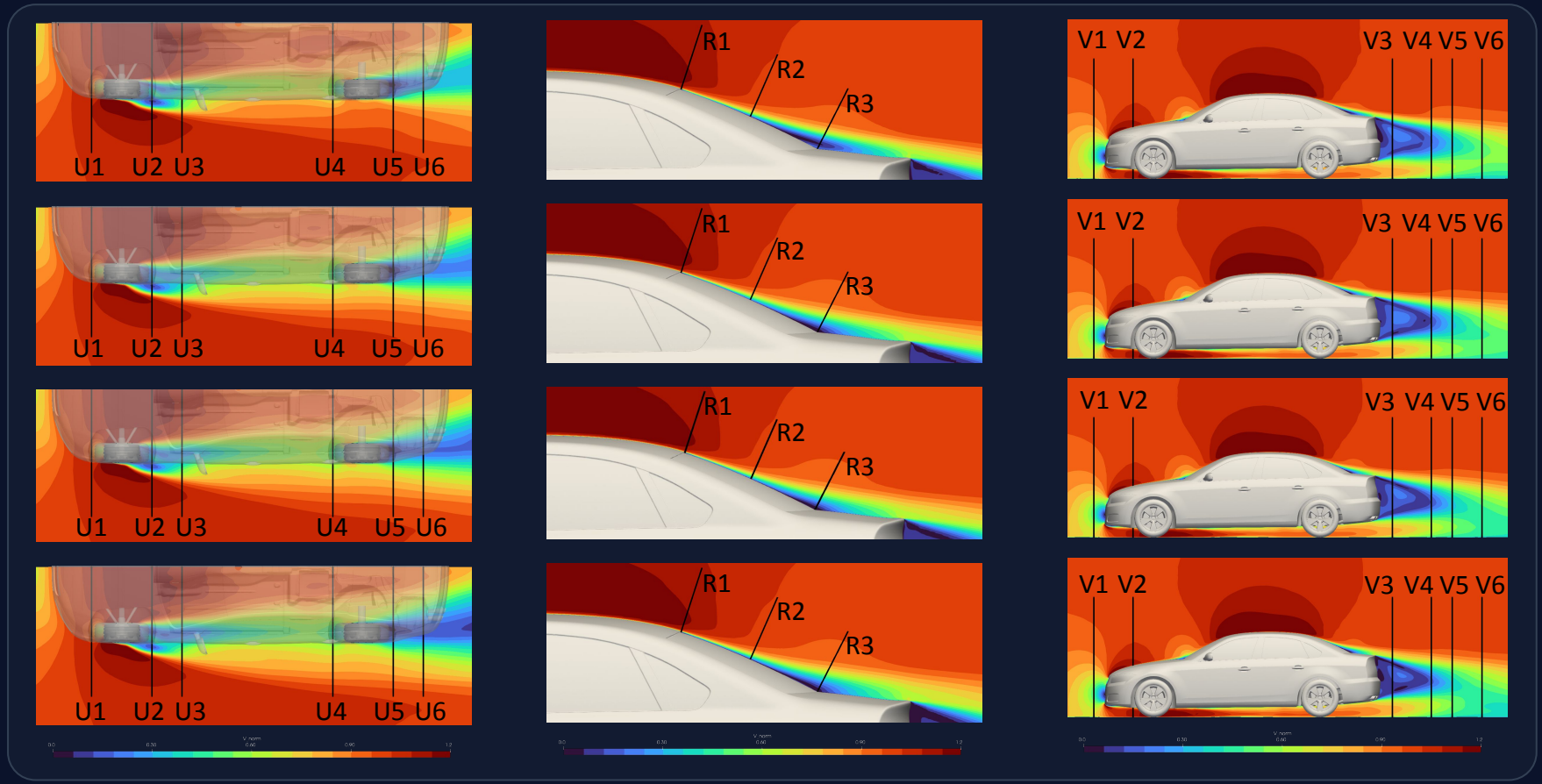
Flow Field — x = 407 mm



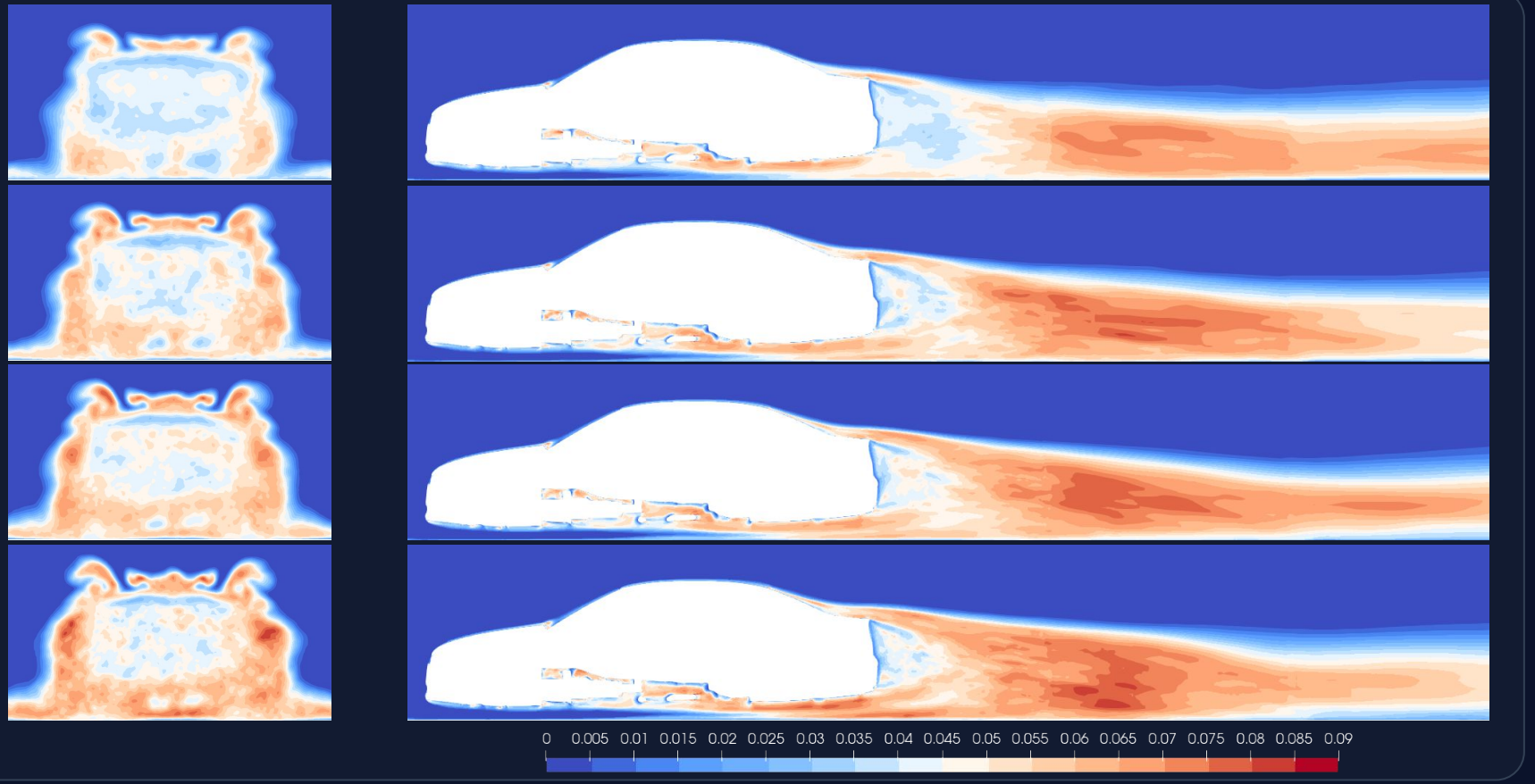
Flow Field — underbody



Velocity profiles



Flow Field — dynamic coefficient



Baseline Mesh

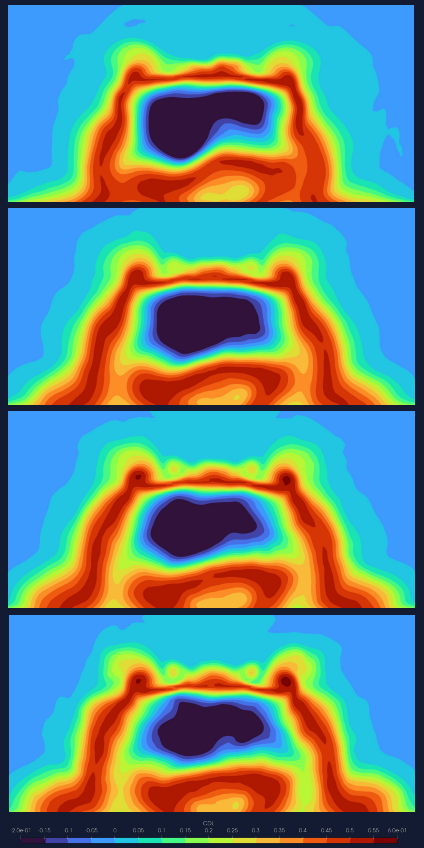
Flow Field — wake X

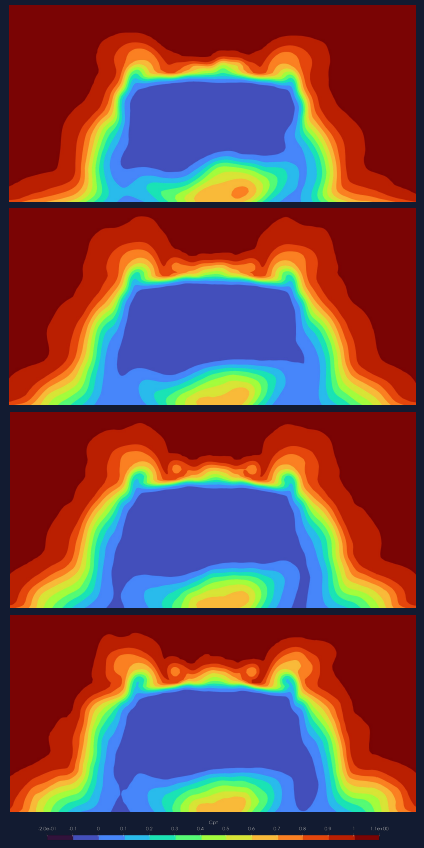
x1

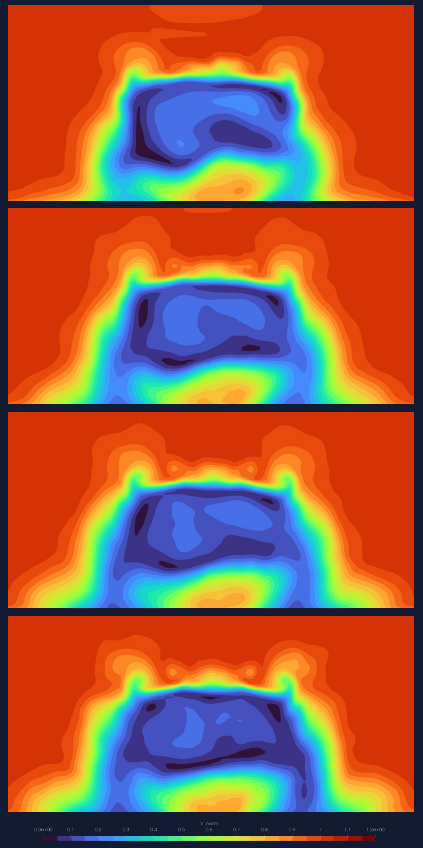
x10

x20

x50







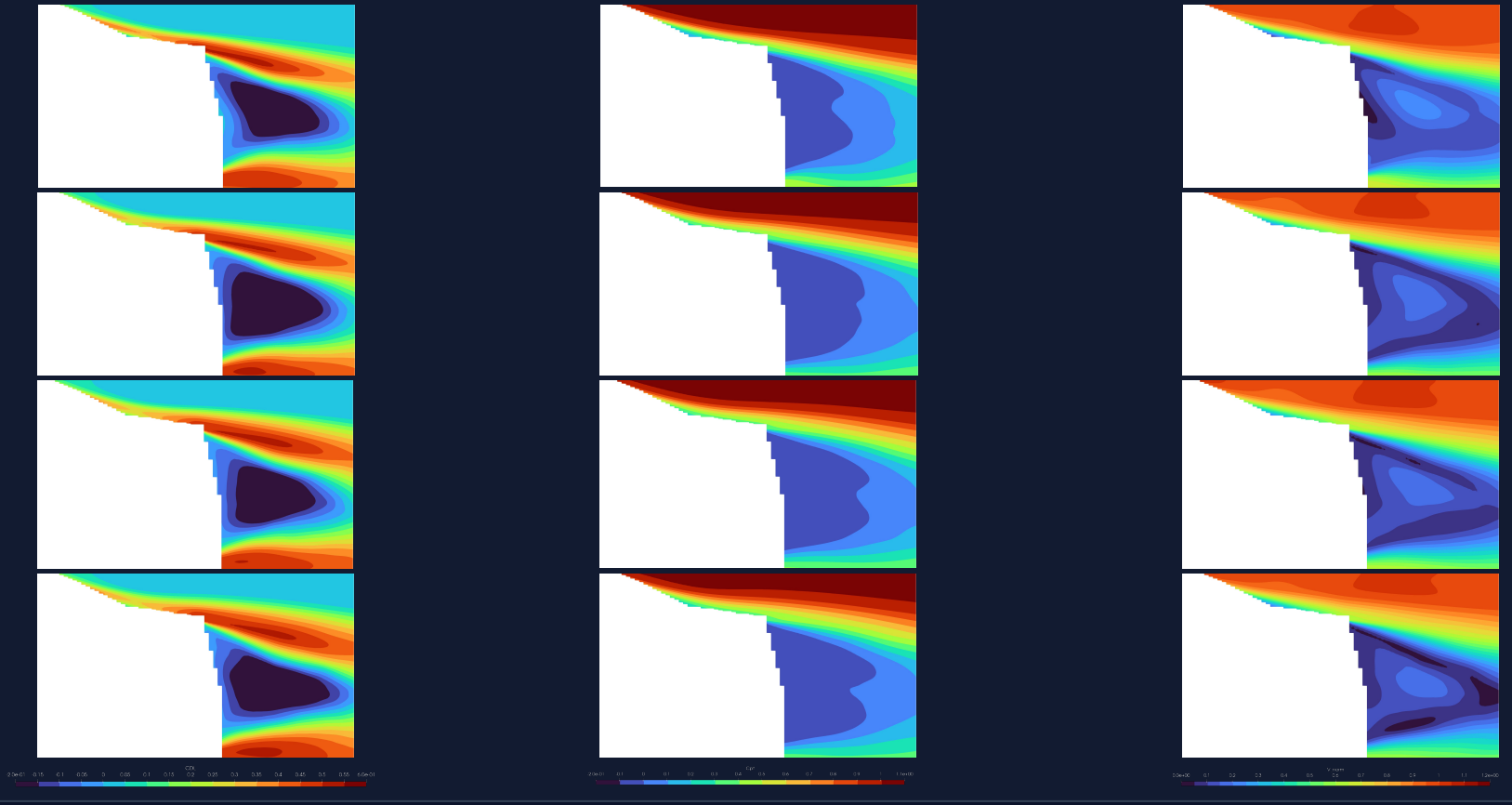
Flow Field — wake Y

x1

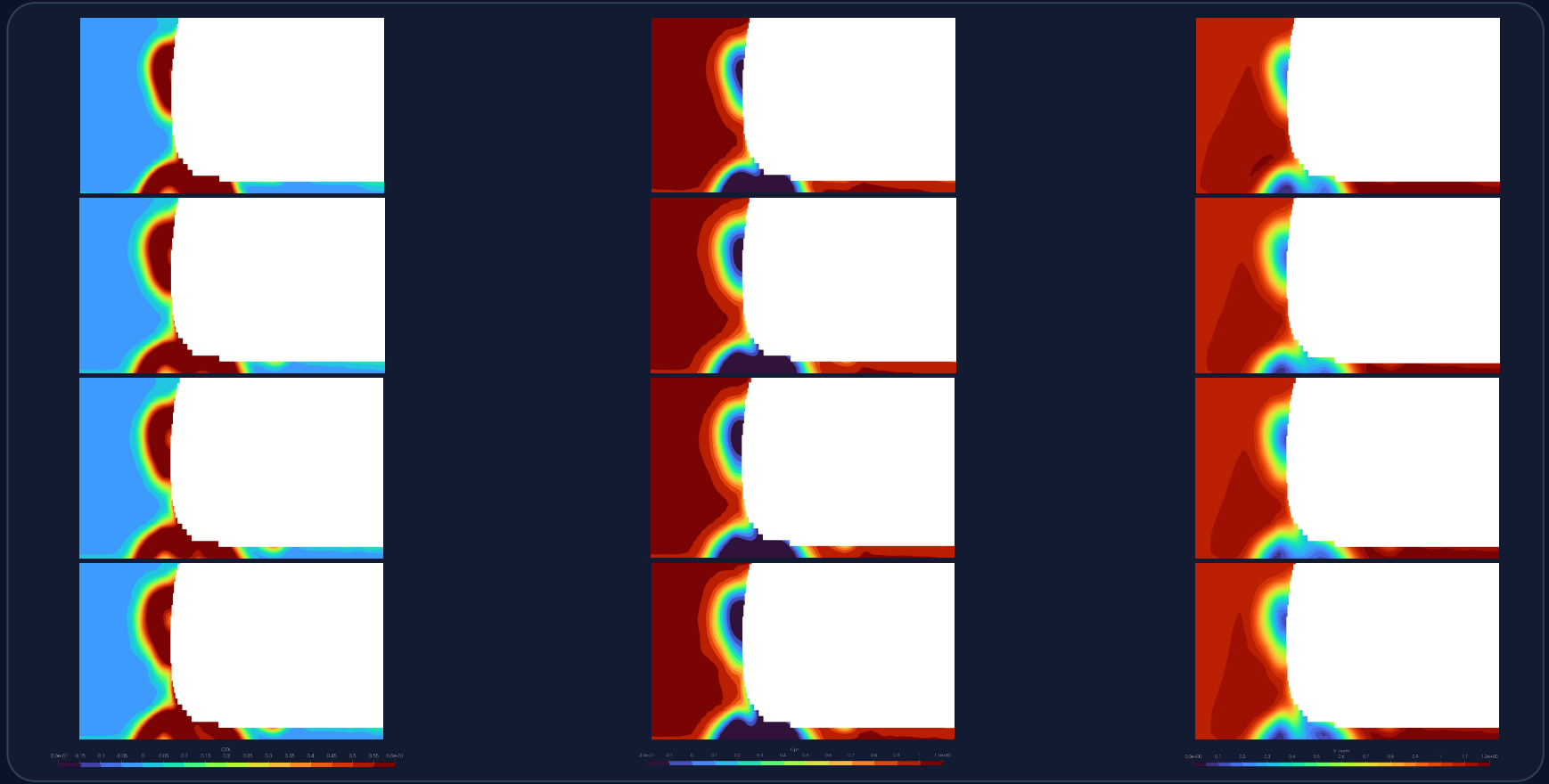
x10

x20

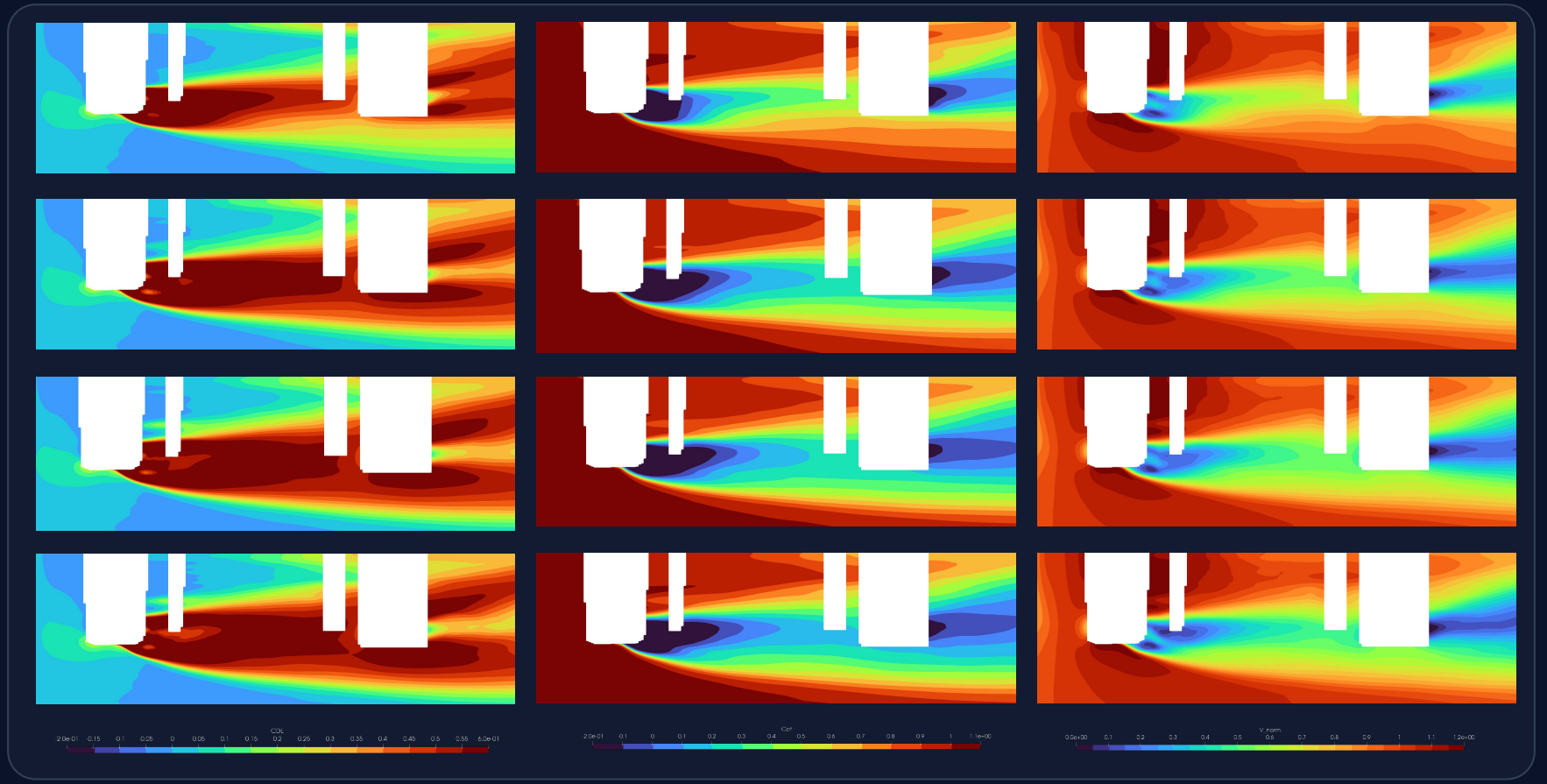
x50



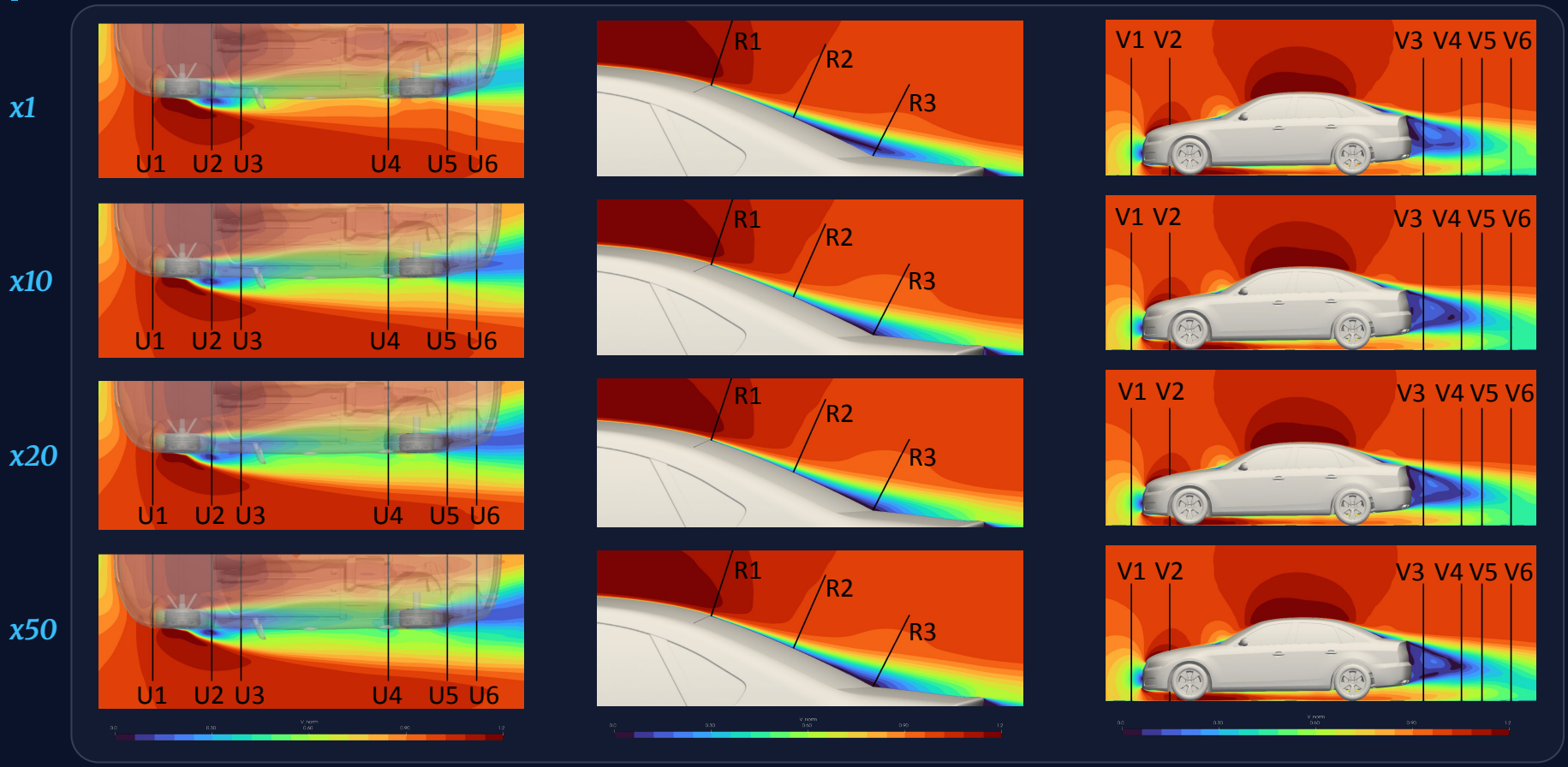
Flow Field — x = 407 mm



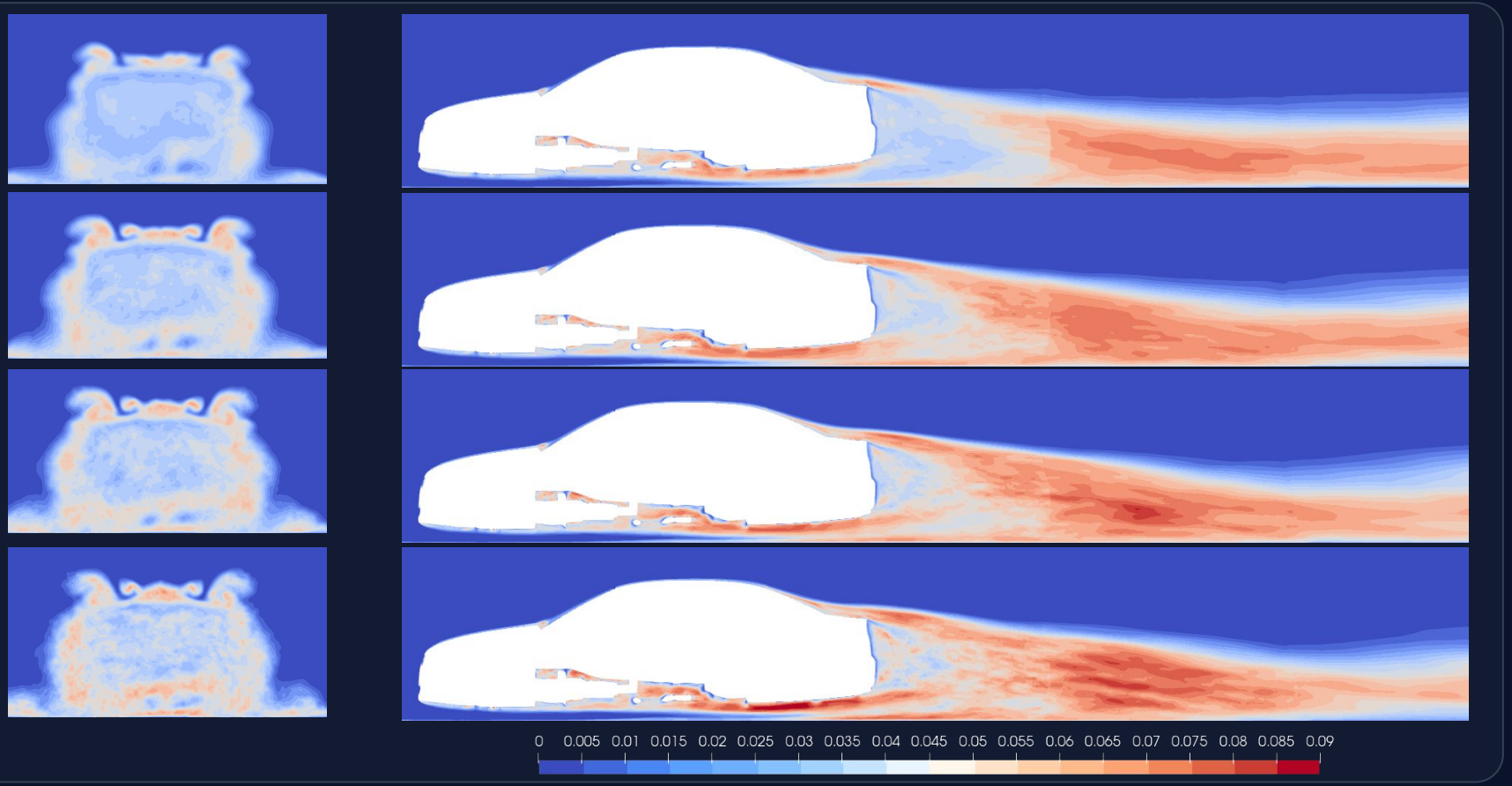
Flow Field — underbody



Velocity profiles

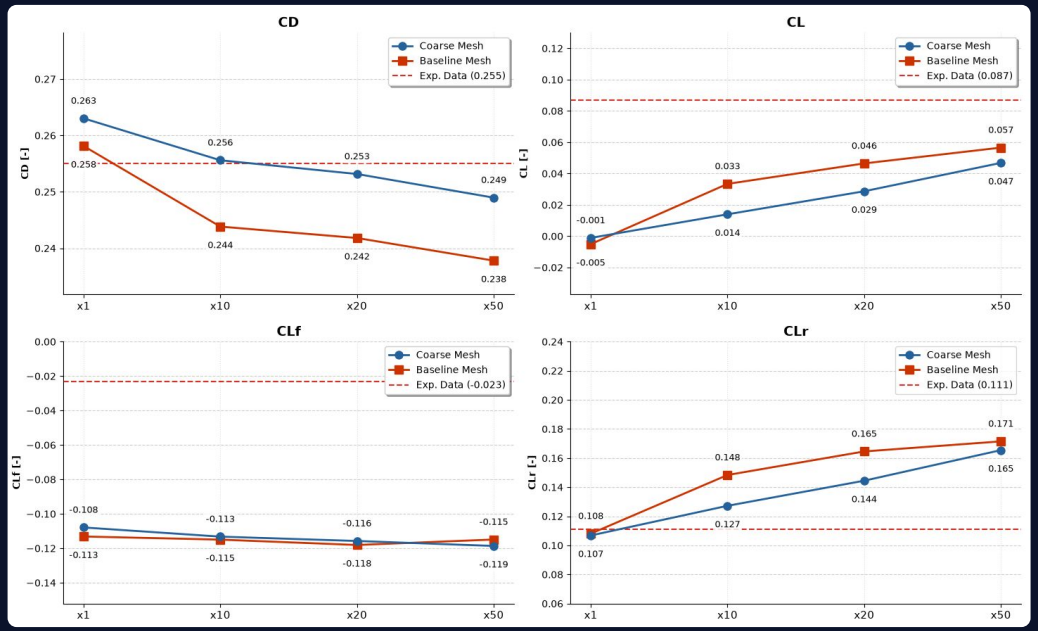


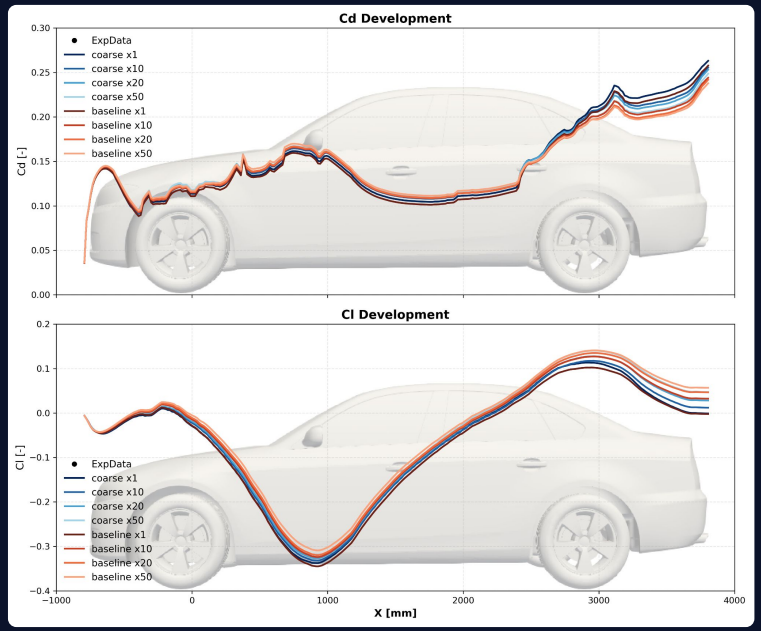
Flow Field — dynamic coefficient



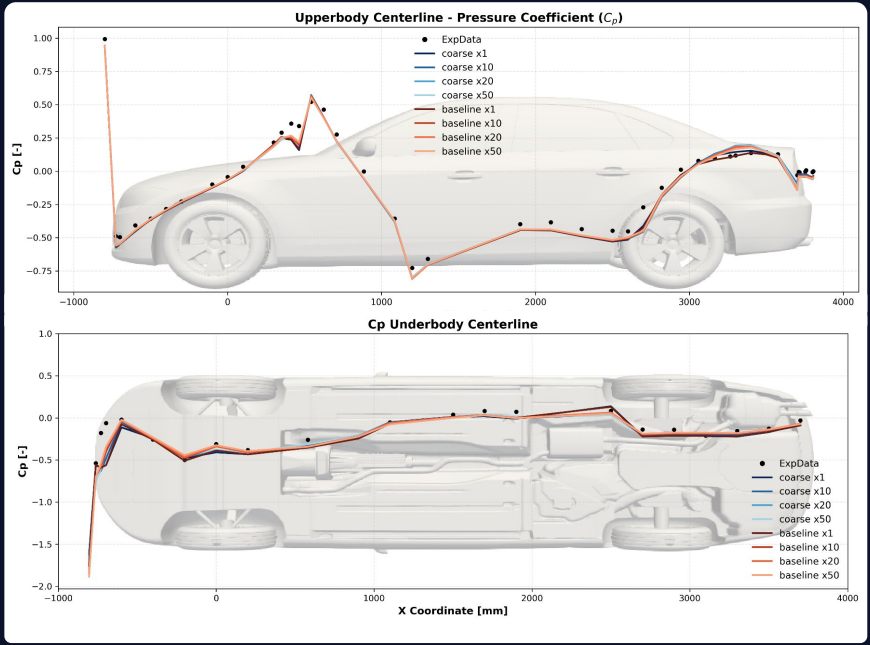
Mesh Comparison

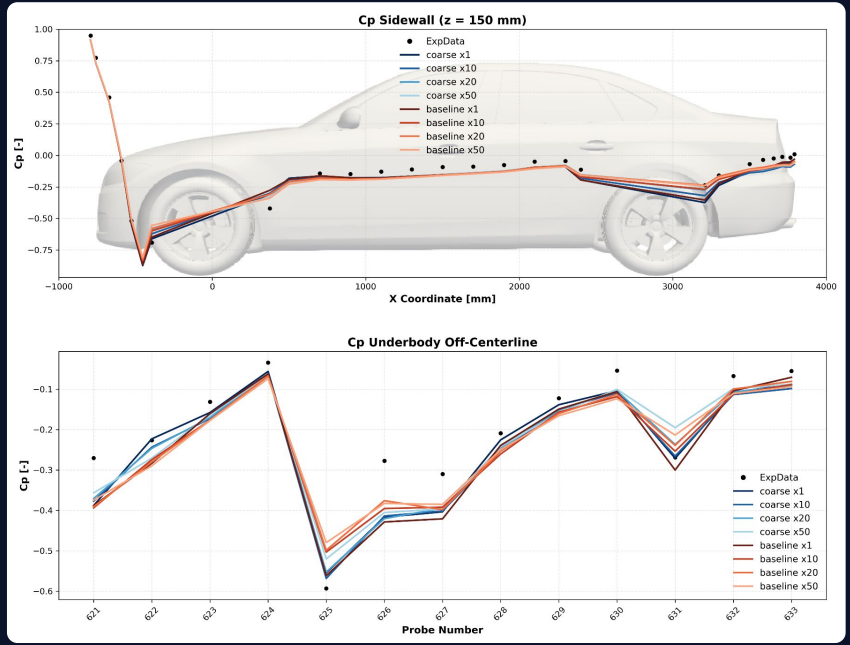
Aerodynamic Coefficients and Developments



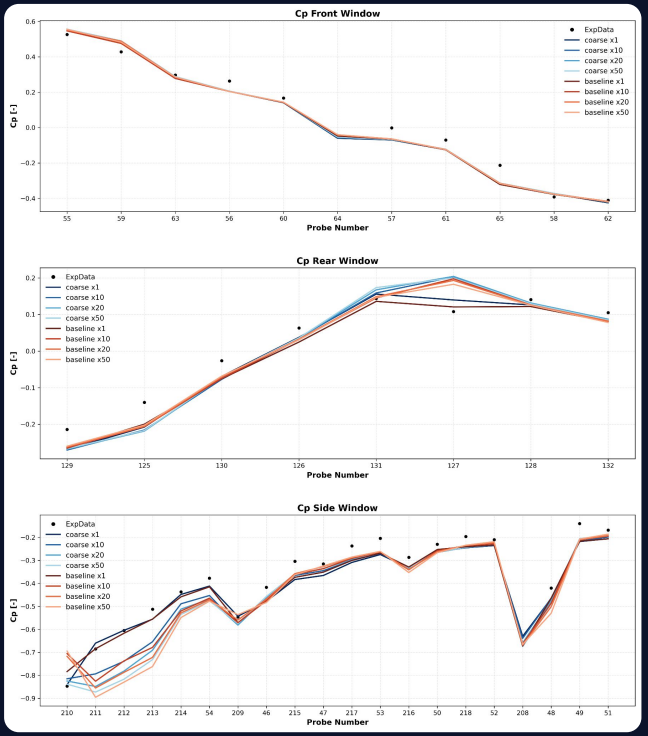


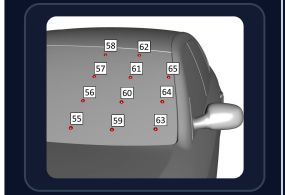
Pressure probes – upperbody, underbody & sidewall



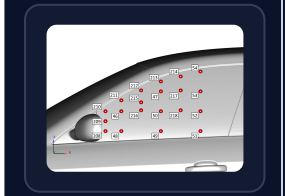


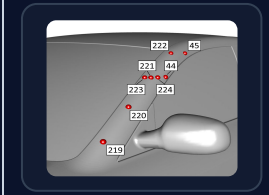
Surface Pressure — windows & pillars

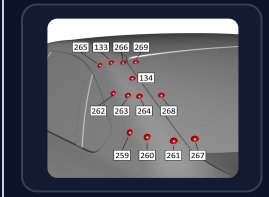




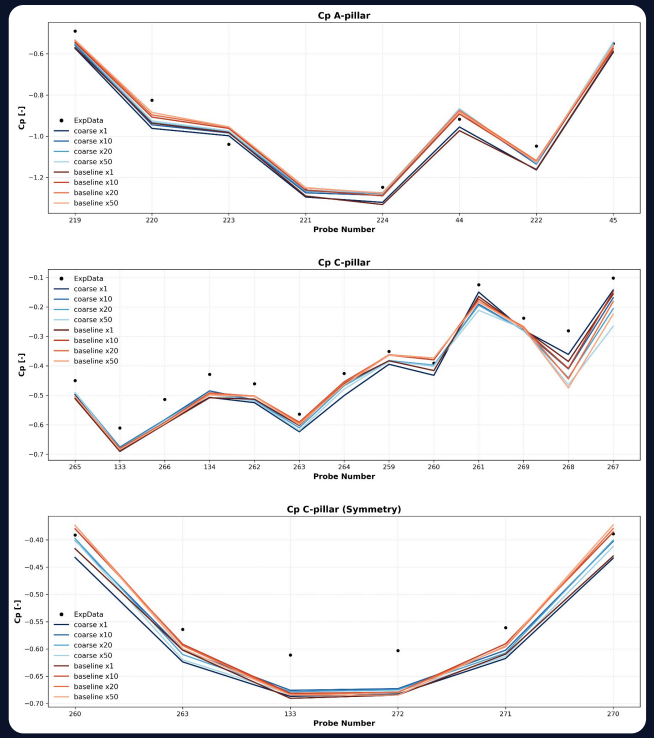




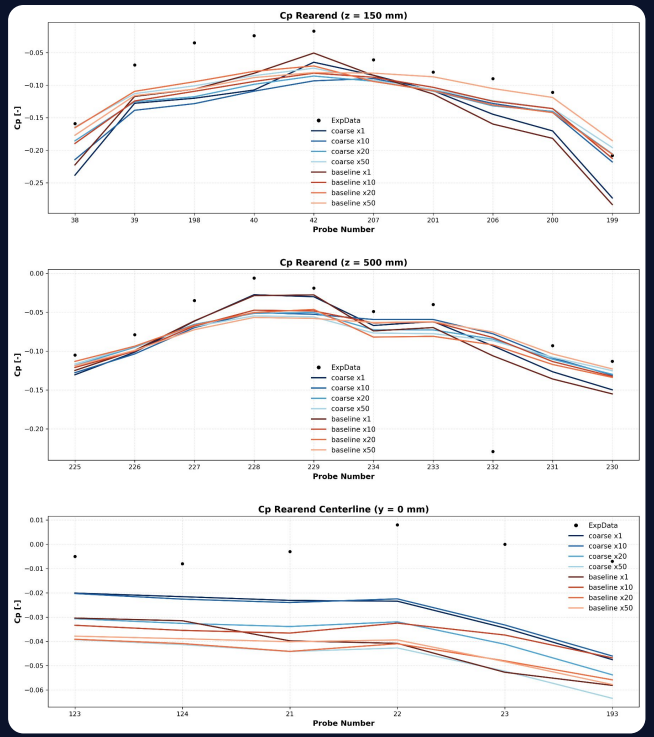


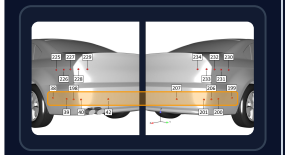


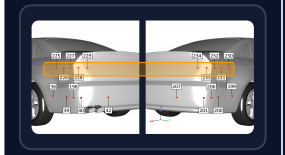




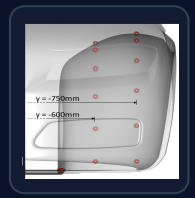
Surface Pressure — rear end & wheelhouse

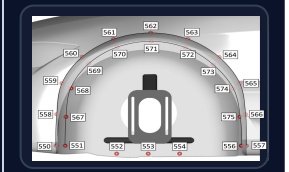


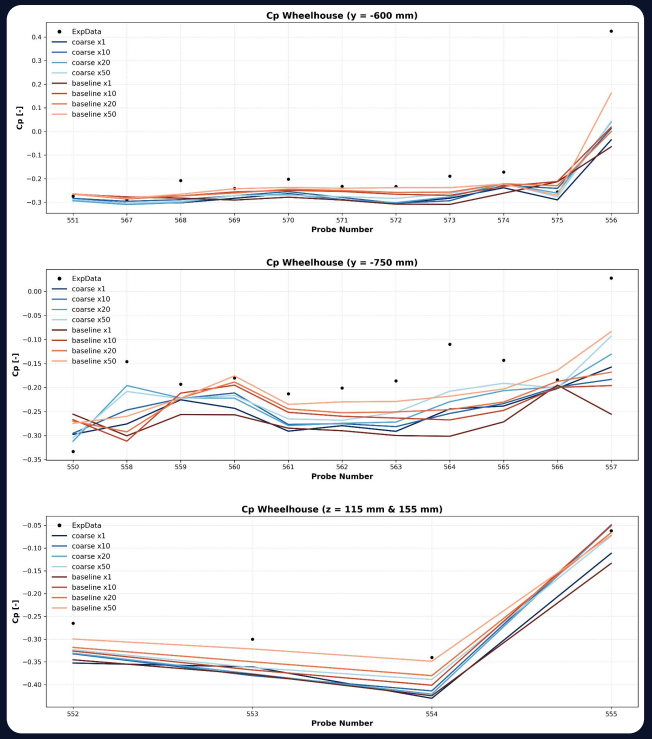




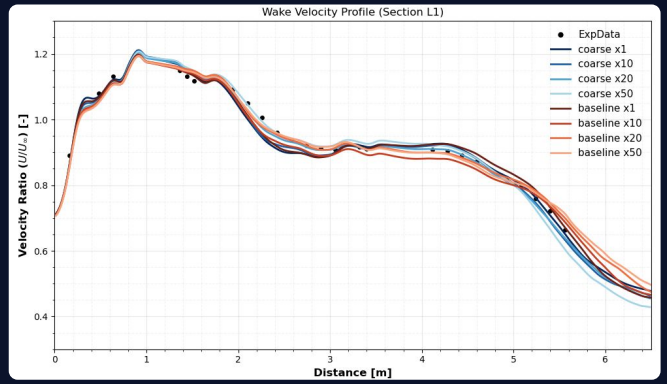


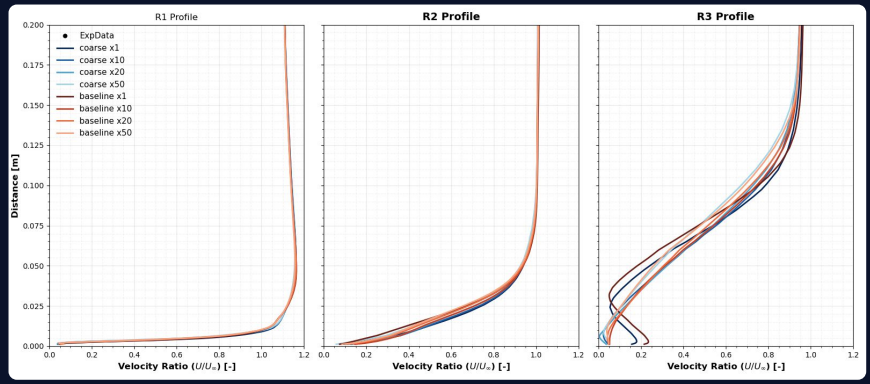


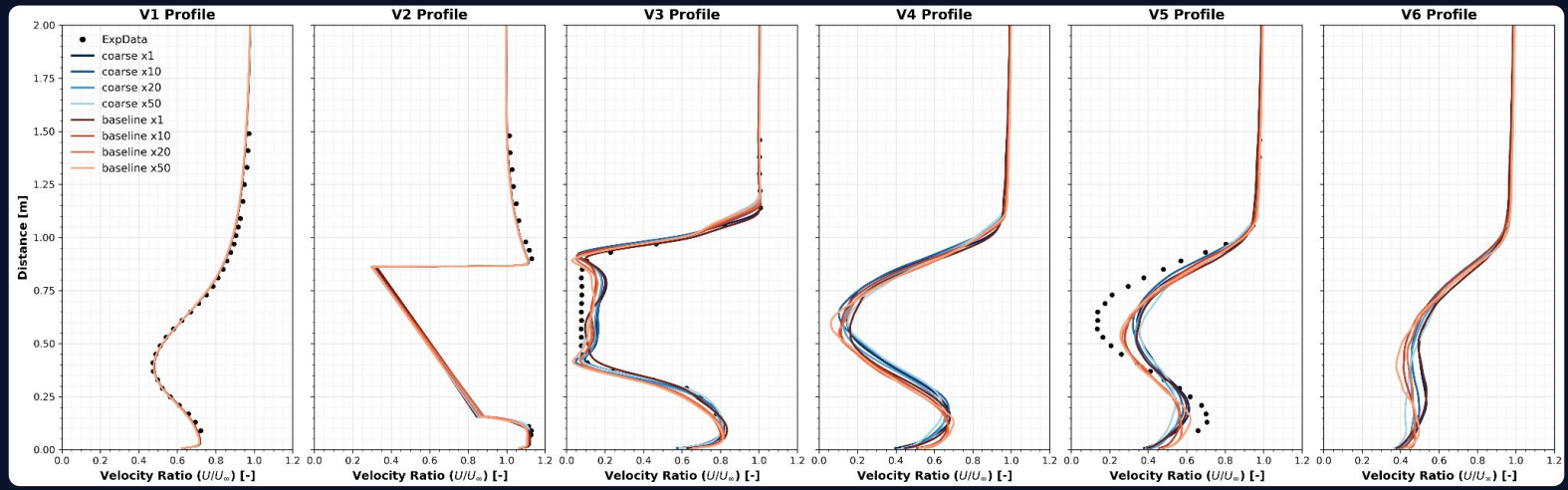




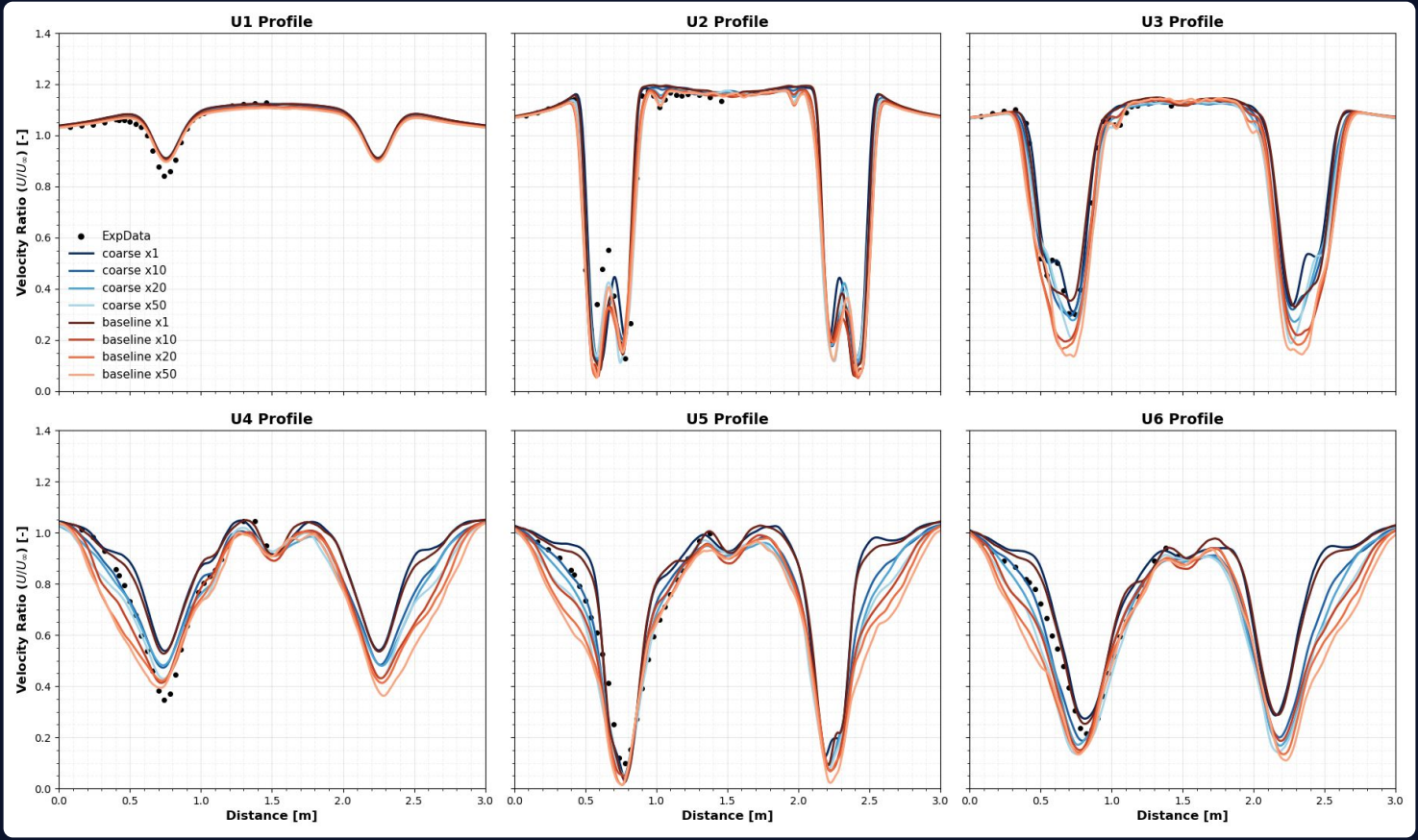
V, L, R – profiles







U – profiles


U1 Profile
U2 Profile
U3 Profile
U4 Profile
U5 Profile
U6 Profile
Velocity Ratio (U/U_∞) [-]
Distance [m]
ExpData
coarse x1
coarse x10
coarse x20
coarse x50
baseline x1
baseline x10
baseline x20
baseline x50